

Dissociated Nonsteroidal Glucocorticoid Receptor Modulators; Discovery of the Agonist Trigger in a Tetrahydronaphthalene–Benzoxazine Series[†]

Mike Barker, Margaret Clackers, Royston Copley, Derek A. Demaine, Davina Humphreys, Graham G. A. Inglis, Michael J. Johnston, Haydn T. Jones, Michael V. Haase, David House, Richard Loiseau, Lesley Nisbet, Francois Pacquet, Philip A. Skone, Stephen E. Shanahan, Dan Tape, Victoria M. Vinader, Melanie Washington, Iain Uings, Richard Upton, Iain M. McLay, and Simon J. F. Macdonald*

RI CEDD, GlaxoSmithKline Medicines Research Centre, Gunnels Wood Road, Stevenage SG1 2NY, United Kingdom

Received March 16, 2006

The tetrahydronaphthalene–benzoxazine glucocorticoid receptor (GR) partial agonist **4b** was optimized to produce potent full agonists of GR. Aromatic ring substitution of the tetrahydronaphthalene leads to weak GR antagonists. Discovery of an “agonist trigger” substituent on the saturated ring of the tetrahydronaphthalene leads to increased potency and efficacious GR agonism. These compounds are efficacy selective in an NFκB GR agonist assay (representing transrepression effects) over an MMTV GR agonist assay (representing transactivation effects). **52** and **60** have NFκB pIC₅₀ = 8.92 (105%) and 8.69 (92%) and MMTV pEC₅₀ = 8.20 (47%) and 7.75 (39%), respectively. The impact of the trigger substituent on agonism is modeled within GR and discussed. **36**, **52**, and **60** have anti-inflammatory activity in a mouse model of inflammation after topical dosing with **52** and **60**, having an effect similar to that of dexamethasone. The original lead was discovered by a manual agreement docking method, and automation of this method is also described.

Introduction

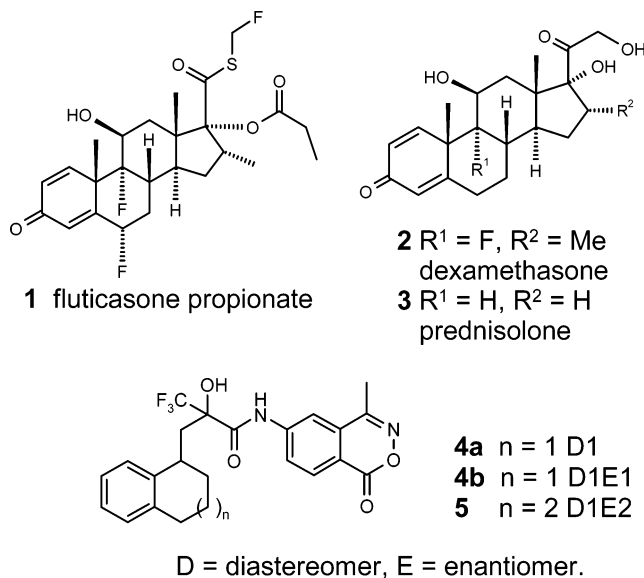
Glucocorticoids have been used for many years as anti-inflammatory agents for treating a whole spectrum of conditions, including asthma and rheumatoid arthritis.¹ Fluticasone propionate **1** is commonly used as a safe and effective inhaled treatment for asthma. In contrast, dexamethasone (**2**) and prednisolone (**3**) are commonly prescribed oral treatments for treating rheumatoid arthritis. About 10 million prescriptions are written each year for oral glucocorticoids in the United States alone, and it is estimated that well over 50% of patients with rheumatoid arthritis are treated more or less continuously with glucocorticoids.² Overall, the market size for glucocorticoids is estimated as \$10 billion per year.³ However prolonged use of orally administered glucocorticoids in the treatment of chronic conditions is blighted by serious and unpleasant side-effects including, among many others, glucose intolerance, muscle wasting, skin thinning, and osteoporosis.

As a consequence of these side effects, there has recently been considerable interest in a hypothesis of selective glucocorticoid agonism where the beneficial anti-inflammatory effects are postulated to derive from transrepression (TR^a) pathways and may be separated from the side effects derived from transactivation (TA) pathways.⁴ Compounds that display selectivity for transrepression over transactivation are often referred to as dissociated agonists. Lucid descriptions of the molecular basis for these pathways have been described in detail elsewhere.^{2–4} Recent publications have described nonsteroidal structures that are dissociated glucocorticoid receptor (GR) agonists that feature both TR/TA selectivity^{5–9} and GR antagonists.^{10,11}

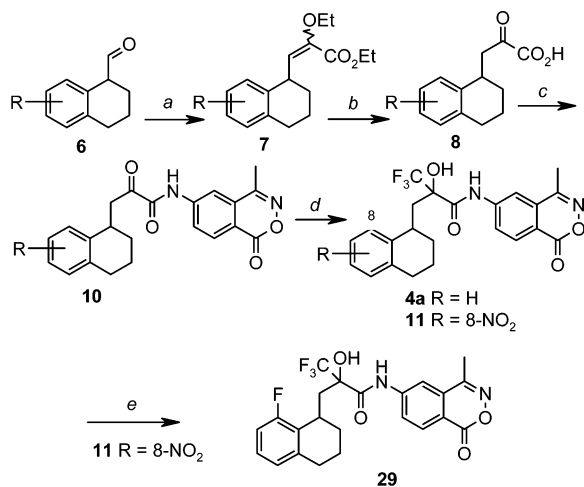
* Corresponding author. Fax: +44 1438-768-302. E-mail: simon.jf.macdonald@gsk.com.

[†] Dedicated to D.A.D. on the occasion of his retirement from GSK, ri CEDD.

^a Abbreviations: GR, glucocorticoid receptor; TR, transrepression; TA, transactivation.



At GSK, we are interested in GR agonists as anti-inflammatory agents and have recently described nonsteroidal GR modulators designed by using an agreement docking method.^{12,13} These modulators, exemplified by **4a**, **4b**, and **5**, are potent binders to GR, with **5** being a sub-micromolar partial agonist. These compounds also possess indications of dissociation, that is, selectivity for transrepression over transactivation. We describe in this paper the discovery of a structural “agonist trigger” that switches this series from being predominantly antagonists and partial agonists of GR into efficacious agonists. This paper also describes the conversion of these leads into potent GR agonists of similar activity to dexamethasone **2**, indications of their efficacy selectivity for TR over TA, nuclear receptor selectivity, and anti-inflammatory activity in vivo after topical dosing to mice. Finally, this paper also describes the automation of the previously manual agreement docking method.

Scheme 1. Method A^a

^a Conditions: (a) (EtO)₂POCH(OEt)CO₂Et, LDA, THF, -10 °C to rt, 18 h, 78% (R = H); (b) TFA:H₂O (3:4), rt, 3 h, used crude; (c) 6-amino-4-methyl-2,3-benzoxazin-1-one **9**, SOCl₂, DMA, -8 to 0 °C, 3 h, 26% (R = H); (d) CF₃TMS, Cs₂CO₃, DMF, 18 h then TBAF (1 M in THF), 30 min 23% (R = H); (e) (i) SnCl₂·2H₂O, THF, 60 °C, 3 h, 82%; (ii) BF₃·OEt₂, DCM, DMF, -15 °C, then add aniline and warm to 5 °C, 14%.

Chemistry

The target compounds were prepared according to the methods shown in Schemes 1–3. Compounds **4a** and **29** were prepared according to method A (Scheme 1) from the appropriately substituted aldehyde **6** (R = H and 8-NO₂, respectively). These were converted in two steps to the α -keto acids **8**, which were then coupled with the known 6-aminobenzoxazinone¹⁴ to afford the pyruvamides **10**. Trifluoromethylation using Ruppert's reagent gave a separable mixtures of the two diastereomers (**4a** and **11**). The 8-nitro derivative **11** was converted into the fluoride analogue **29** by a sequence of reduction, diazotization, and fluorination.

A much quicker, more general route (method B) was subsequently designed for tetrahydronaphthalene featuring substitution on the aromatic ring (Scheme 2). This was used to prepare analogues **17**–**28**. Thus, the target compounds were prepared convergently in three steps from an appropriately substituted tetralone and a trifluoromethylpyruvamide hydrate **12** as a common intermediate. The trifluoromethylpyruvamide hydrate **12** was prepared in a three-stage sequence from the aminobenzoxazinone **9**¹⁴ by formylation followed by dehydration to the isonitrile and, finally, in a Passerini reaction, treatment with trifluoromethylacetic anhydride. The required substituted methylene tetralins **14** were prepared from the correspondingly substituted tetralones **13** via treatment with methyltriphenylphosphonium bromide in a Wittig reaction or using the Tebbe reagent (μ -chloro- μ -methylene[bis(cyclopentadienyl)titanium]dimethylaluminum).

Thermal ene reactions between the methylene tetralins **14** and the trifluoromethylpyruvamide hydrate **12** provided the coupled products **15** in good to excellent yields. Last-stage reduction of the trisubstituted double bond in **15** proved very difficult in part due to its hindered nature and in part due to the ease of reduction of the benzoxazinone. Generally applicable conditions were found, eventually utilizing diimide generated using microwaves from an excess of tosyl hydrazide. Reduction using alternative sources of diimide such as mesitylsulfonyl hydrazide failed. The resultant diastereomers **16** were obtained in low to moderate yields and were generally separated using reverse phase HPLC. The racemic diastereomers were tested and compounds of

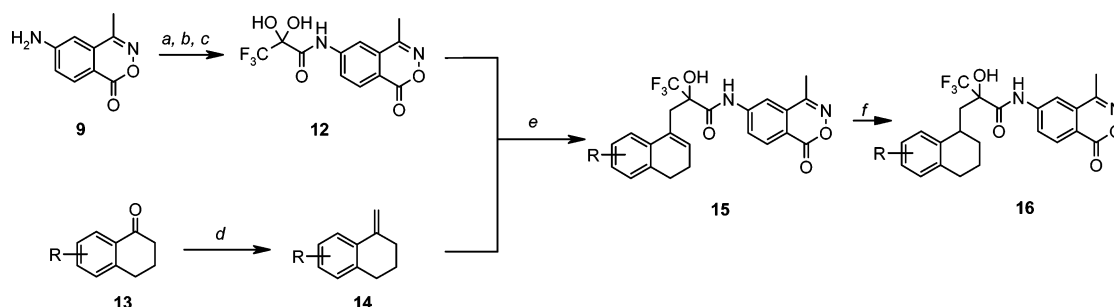
particular interest were separated into their component enantiomers. The diastereomers were assigned as diastereomer 1 (D1) or diastereomer 2 (D2) on the basis of their retention times on reverse phase LC/MS. Thus D1 was assigned as the faster eluting (more polar) isomer and D2 assigned as the slower eluting (less polar) isomer. Subsequently analysis of the ¹H NMR spectra confirmed that all the isomers had been consistently assigned on the basis of the coupling pattern exhibited by one of the protons of the chain CH₂ (Figure 1).

The enantiomers were assigned as enantiomer 1 (E1) and enantiomer 2 (E2) on a similar basis of retention times on chiral HPLC. Thus, the faster eluting enantiomer was assigned as E1 and the slower eluting enantiomer as E2. It is assumed that the most active enantiomers for the various analogues share similar absolute chirality, but no evidence was gathered to confirm this assumption (see Table 1 for examples).

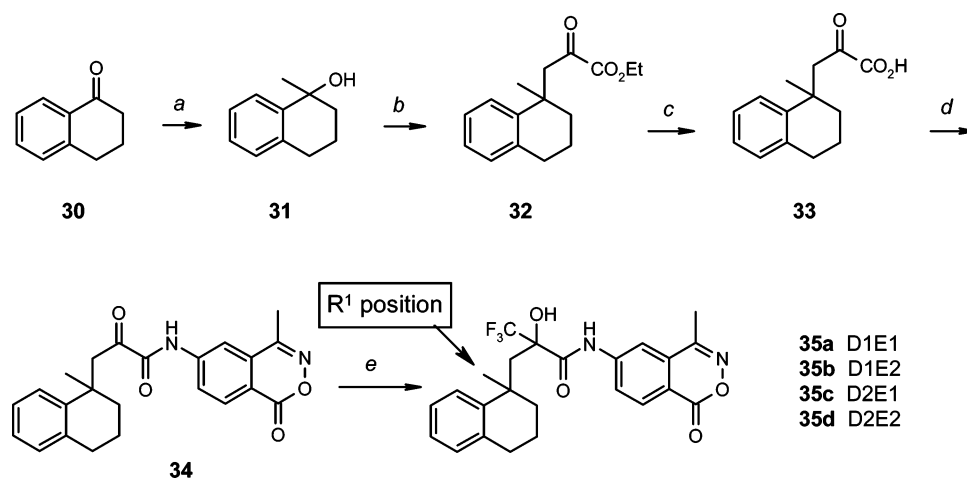
Several routes were used for analogues that feature variation in the R¹ position (Schemes 3 and 4). Initially, the R¹ = Me analogues **35a**–**35d** were prepared via the carbinol **31**, which is available from tetralone **30**. Reaction of the carbinol **31** with the silyl enol ether of pyruvate in the presence of tin(IV) chloride gave the pyruvate **32** in modest yield. The remainder of the route is as described previously (Scheme 1). In the last step, introduction of the trifluoromethyl group into **34** proved capricious and very low yielding. The R¹ = Et tetrahydronaphthalene **36** and suberan analogue **42** were prepared similarly (shown in Table 2). Nitration of **36** with a K₁₀ montmorillonite clay complex with copper(II) nitrate and acetic anhydride afforded a mixture of isomeric products **39**–**41** that are separable by flash chromatography and HPLC.

A more versatile route was subsequently developed allowing variation of the R¹ group on the congested quaternary carbon, even including substituents such as *tert*-butyl (Scheme 4). This route featured as the key step a palladium cascade reaction,¹⁵ which involves three transformations in one vessel exemplified by the transformation of **47** to **48**. Thus an aryl iodide with a tethered alkene **47** initially undergoes an intramolecular cyclization under palladium catalysis to form the saturated ring of the tetrahydronaphthalene. The resultant palladium intermediate is subsequently trapped with carbon monoxide followed by a furylstannane to afford **48**.

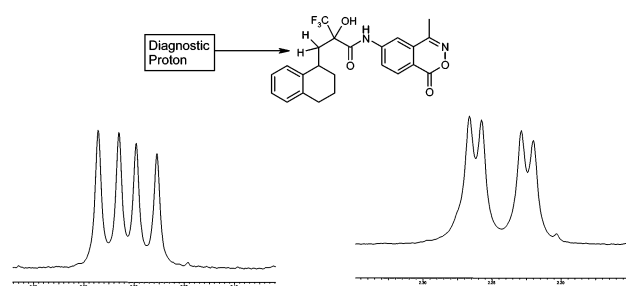
The route is exemplified for the synthesis of the 1-ethylpropyl R¹ analogue (Scheme 4). Preparation of the cascade reaction precursor **47** commences from commercially available *o*-iodobenzylzinc bromide **43**, 1-ethylpropylzinc bromide, and acryloyl chloride **44**. In a one-pot procedure, the acryloyl chloride **44** is first converted to the desired vinyl ketone **45** using 1-ethylpropylzinc bromide and a palladium catalyst followed by in situ reaction of the vinyl ketone with *o*-iodobenzylzinc bromide to afford **46** in 36% yield. This one-pot procedure telescopes two steps originally described by Rieke and co-workers.¹⁶ Conversion of the ketone **46** to the olefin **47** was accomplished using the standard Wittig procedure in 76% yield. Heating **47** in the presence of palladium acetate, triphenylphosphine and 2-furyltributylstannane under an atmosphere of carbon monoxide in toluene then gave **48** in 20% yield after chromatography. Ozonolysis of the furan gave a mixture of the ketoacid **49** and acid **50**, where a carbonyl group has been extruded. This mixture was then coupled with the benzoxazine **9** using the conditions described earlier to give **51** in 33% yield for the two steps. The trifluoromethylation was achieved in this instance using cesium fluoride and Ruppert's reagent in DMF and gave an 81% yield of two diastereomers from which **52** D2E2 was separated. Separation of the diastereomers and

Scheme 2. Method B^a

^a Conditions and notes: (a) HCO₂H, Ac₂O, 55 °C, 2 h then 6-amino-4-methyl-2,3-benzoxazin-1-one **9**, THF, rt, 2 days, used crude; (b) POCl₃, Et₃N, THF:DMPU (2.5:1), rt, 2 days, 67%; (c) trifluoroacetic anhydride, rt, 2 days then MeOH, 87%; (d) Wittig or Tebbe reactions, good yields; (e) 200 °C, 10 min, good to excellent yields; (f) excess TsNHNH₂, NMP, 150 °C, microwave, 30 min, low yields.

Scheme 3. Method C^a

^a Conditions: (a) MeLi, CeCl₃, THF, -70 °C, 2 h, 46%; (b) methyl 2-(trimethylsilyloxy)acrylate, SnCl₄, CHCl₃, -60 °C, 17%; (c) KOH, MeOH, room temperature, 2 h, used crude; (d) SOCl₂, DMA, -5 °C, then **9** (Scheme 2), warm to room temperature, 3 h, 67%; (e) TMSCF₃, Cs₂CO₃, DMF, 3 h then TBAF, 30 min, 2.5%.



Diastereomer 1 ($J = 15.2, 8.3 \text{ Hz}$) Diastereomer 2 ($J = 15.2, 3.5 \text{ Hz}$)

Figure 1. Details of a representative ¹H NMR spectra (in CDCl₃) for the compounds listed in Table 1 illustrating the coupling differences for one of the protons in the chain CH₂ for diastereomer 1 and diastereomer 2 appearing between δ 2.20–2.30. The diastereomers in Table 1 were assigned consistently on this basis.

enantiomers was achieved using standard purification techniques. The yields described for this sequence are representative for the compounds described in Table 3 apart from the capricious last stage trifluoromethylation, where yields varied from good to poor (5–81%). Despite considerable optimization work, we were unable to discover a general set of trifluoromethylation conditions that consistently gave good yields of products for a range of substrates. Compounds **52–62** were prepared according to this route.

Crystals of the enantiomer (D2E1) of **60** were grown by slow evaporation of an ethanol solution allowing determination of

its absolute stereochemistry by single-crystal X-ray diffraction as *SS*. Therefore, the absolute stereochemistry of **60** (D2E2) is *RR*.

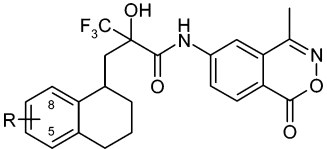
Biological Assays

GR Binding Assay. The compounds were tested for their ability to bind to GR using competition experiments with fluorescent-labeled dexamethasone.¹² The tight binding limit of the assay is about $\text{pIC}_{50} = 8.5$.

GR NF κ B Functional Agonist Assay (Transrepression). A functional GR agonist assay was carried out using human A549 lung epithelial cells engineered to contain a secreted placental alkaline phosphatase gene under the control of the distal region of the NF κ B-dependent ELAM promoter.¹⁷ This assay allows determination of the ability of compounds to repress transcription (i.e. transrepression). Efficacy is expressed as a percentage of the dexamethasone response.

GR MMTV Functional Assay (Transactivation). Human A549 lung epithelial cells were engineered to contain a renilla luciferase gene under the control of the distal region of the LTR from the mouse mammary tumor virus as previously described.¹² While the standards dexamethasone (**2**) and prednisolone (**3**) have comparable efficacy in the NF κ B transrepression agonist assay and the MMTV transactivation agonist assay, they are more potent in the NF κ B assay by about 0.4–0.6 pIC_{50} units.

GR MMTV Antagonist Assay. The GR antagonist assay also used human A549 lung epithelial cells stably transfected

Table 1. Biological Data for Analogues Featuring Substitution of the Aromatic Ring of the Tetrahydronaphthalene


compd	R	stereo. ^a	pIC ₅₀		
			GR binding ^{b,c}	NFκB ^{b,d} (% max)	MMTV antagonism ^{b,e}
2	—	—	8.10 ± 0.04	8.93 ± 0.07 (110 ± 5)	<5
3			nt ^g	8.07 ± 0.15 (98.4 ± 3.8)	nt
RU486 ^f			8.24 ± 0.09	<6 (4 ± 2)	8.33 ± 0.36
4a	H	D1 rac	8.1 ± 0.17	<6 (35 ± 2)	nt
17	5-OMe	D1 rac	7.9 ± 0.05	<6 (66 ± 13)	nt
18	5-CN	D1 rac	7.8 ± 0.08	<6 (68 ± 16)	nt
19a	5-Me	D1 rac	7.7 ± 0.06	<6 (92 ± 10)	6.1 ± 0.15
19b	5-Me	D1E1	8.5 ± 0.01	<6 (98 ± 1)	6.7 ± 0.02
20a	5-Cl	D1 rac	7.8 ± 0.04	<6 (94 ± 25)	nt
20b	5-Cl	D1E1	8.3 ± 0.03	<6 (99 ± 18)	6.4 ± 0.03
21	5-F	D1 rac	7.8 ± 0.14	<6 (78 ± 14)	6.3 ± 0.11
22	5-NH ₂	D1 rac	7.6 ± 0.08	<6 (32 ± 18)	5.7 ± 0.06
23a	5-Br	D1 rac	7.8 ± 0.12	<6 (105 ± 7)	6.1 ± 0.03
23b	5-Br	D2 rac	7.4 ± 0.09	<6 (81 ± 30)	nt
23c	5-Br	D1E1	8.2 ± 0.25	<6 (86 ± 21)	nt
23d	5-Br	D1E2	6.0 ± 0.11	<6 (67 ± 6)	nt
23e	5-Br	D2E1	7.6 ± 0.10	<6 (53 ± 31)	nt
23f	5-Br	D2E2	6.2 ± 0.05	<6 (47 ± 4)	nt
24	5-NO ₂	D1 rac	7.9 ± 0.19	<6 (52 ± 23)	nt
25	6-NO ₂	D1 rac	6.9 ± 0.07	<6 (35 ± 22)	nt
26	7-NO ₂	D1 rac	7.7 ± 0.42	<6 (42 ± 2)	nt
27	6-F	D1 rac	7.9 ± 0.08	<6 (74 ± 16)	nt
28	7-F	D1 rac	7.8 ± 0.06	<6 (63 ± 17)	nt
29	8-F	D1 rac	7.5 ± 0.24	<6 (42 ± 16)	nt

^aD = diastereomer, E = enantiomer. The stereochemistry of the diastereomers has been consistently assigned by ¹H NMR. Enantiomer assignment is based on the order of elution from analytical chiral HPLC. See the text for further details. ^bpIC₅₀ values are from duplicate wells with at least *n* = 3 from 11 point dose–response curves with a top concentration of 10 mM. Standard errors are shown. ^cIn the GR binding assay, compounds were tested for their ability to bind to GR using competition experiments with fluorescently labeled dexamethasone. ^dThe NFκB assay used human A549 lung epithelial cells engineered to contain a secreted placental alkaline phosphatase gene under the control of the distal region of the NFκB-dependent ELAM promoter. With a top concentration of 10 mM being tested, pIC₅₀'s are not quoted for values <6. All the compounds listed apart from dexamethasone had pIC₅₀ values <6 and are not shown. Maxima are quoted with reference to the maximum for dexamethasone (**2**) (the standard used). ^eThe GR antagonist assay used human A549 lung epithelial cells stably transfected with the mouse mammary tumor virus (MMTV) luciferase reporter gene. Compounds were tested for their ability to antagonize dexamethasone-induced activation. ^fRU486 (mifepristone) was used as the standard for GR antagonism. ^gnt = not tested.

with the mouse mammary tumor virus (MMTV) luciferase reporter gene. Compounds were tested for their ability to antagonize dexamethasone-induced activation.¹⁷ This assay also allows determination of the ability of compounds to activate transcription (i.e. transactivation). Data for target compounds and standards [dexamethasone for agonism and mifepristone (RU486) for antagonism] in these assays are reported.

Topical Mouse DTH Assay. Anti-inflammatory effects were determined in mice using an oxazolone-induced mouse ear skin delayed types hypersensitivity model.¹⁸ Balb/c mice were sensitized with oxazolone and after 5 days the compounds were applied topically to the right ear only. Oxazolone was then applied topically to both ears 1 h later followed 3 h postchallenge with further treatment with compound to the right ear only.

Twenty-four hours later the thickness of each ear was measured and an ED₅₀ calculated.

Results and Discussion

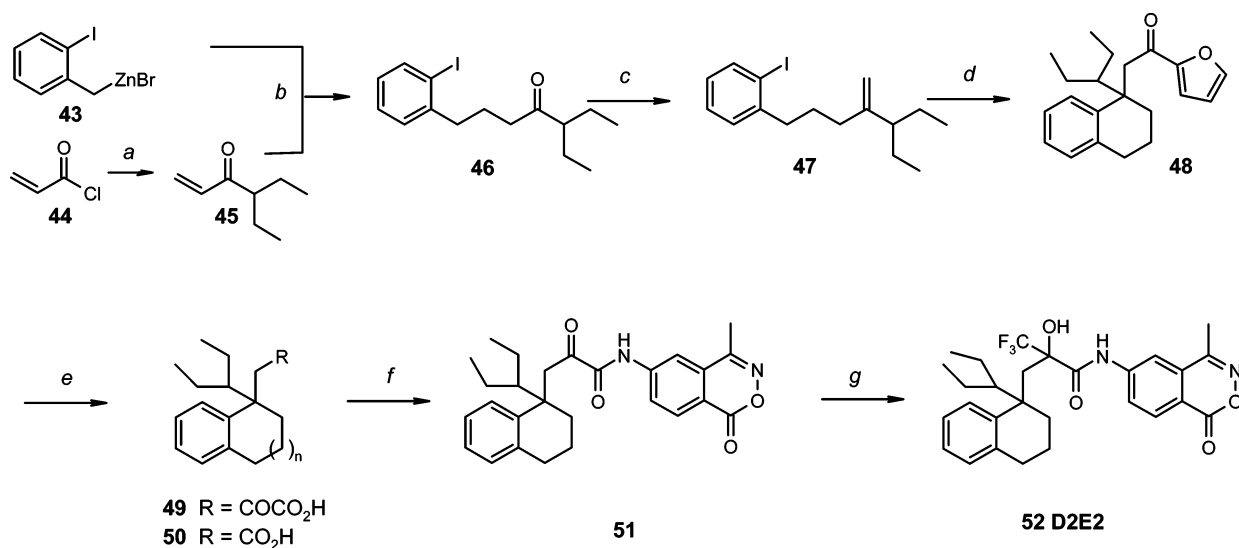
We have previously described the discovery of the tetrahydronaphthalene **4b** and suberan **5** as GR modulators using an “agreement docking method” with **5** being a partial agonist possessing micromolar levels of potency.¹² Our next aim was to increase the levels of GR agonist potency and efficacy to those similar to dexamethasone **2**, a compound widely used in the clinic. We were also keen to evaluate whether this nonsteroidal series would offer any selectivity for transrepression over transactivation. As other nonsteroidal series have shown a profound influence of aromatic substituents on biological activity,^{5,6} we decided to explore the effect of a wide variety of substituents at each position of the aromatic ring of the tetrahydronaphthalene. We chose to work in the tetrahydronaphthalene series rather than the suberan series,¹² due to the greater availability of starting materials and the synthetic accessibility of the targets. A comprehensive list of analogues was prepared represented by those shown in Table 1, and in general, at least one isomer of each analogue displays good GR binding activity. However, no appreciable agonism of GR was observed, although hints of activity appear at high concentrations (see the percentage maxima, Table 1); these may also be the result of cell toxicity. In general the D1 analogues are more potent binders than D2 analogues (data only shown for the 5-bromo derivative **23a** vs **23b** and **23c** vs **23e**). As might be expected, one enantiomer of the active diastereomer (D1E1, **23c**) is slightly more potent than the other enantiomer (D1E2, **23d**). Surprisingly, one enantiomer of the other diastereomer (D2E1, **23e**) is also a good binder, although this has been rationalized by modeling studies¹² that suggest that the stereochemistry of the alcohol is preserved and that it is the stereochemistry at the quaternary carbon of the tetrahydronaphthalene that changes. These trends, illustrated for the 5-bromo analogue **23**, generally also apply for the variety of substituents at the 5-, 6-, 7-, or 8-position. In general, the SAR obtained from data generated on the diastereomers is representative of that found with the corresponding single enantiomers (as can be seen with **23**) with the enantiomers typically being more potent in the binding assay (see for example **19a** and **19b** or **20a** and **20b**).

A broad range of substituents are tolerated, as shown by the 5-substituted analogues **17–24**. Electronic, steric, or polar differences make little difference to the binding, although there is a correlation between increasing lipophilicity and higher percentage maxima in the NFκB assay; for example, the percentage maxima for the 5-NH₂ (**22**) and 5-Br (**23a**) analogues are 32% and 105%, respectively.

The 5-substituted analogues are as potent as or slightly more potent than the corresponding 6-, 7-, or 8-substituted analogues: compare the 5-F analogue **21** with the 6-, 7-, or 8-F analogues **27–29**, and the 5-NO₂ analogue **24** with the 6- and 7-NO₂ analogues **25** and **26**. This trend also applies with other substituents (data not shown).

The more potent binders **19a**, **19b**, **20b**, and **23a**, including the very small 5-fluoro analogue **21**, are sub-micromolar GR antagonists as determined in the MMTV antagonism assay. As will be seen later, substitution on the aromatic ring of the tetrahydronaphthalene is a powerful switch for converting GR agonists into antagonists.

With little success in discovering GR agonism through substitution of the aromatic ring of the tetrahydronaphthalene, it was decided to explore modification of the saturated ring of

Scheme 4. Method D^a

^a Conditions: (a) 1-ethylpropylzinc bromide, Pd(PPh₃)₄, THF, 0 °C, 1.5 h, then added to (b) LiCl, CuCN, **43**, TMSCl, -70 °C to rt, 2 h, 36%; (c) MePPh₃Br, *n*-BuLi, THF, reflux, 18 h, 76%; (d) Pd(OAc)₂, PPh₃, 2-furyltributylstannane, CO, PhMe, reflux, 3 h, 20%; (e) O₃, MeOH, -78 °C, 1 h, then KOH, MeOH, 1.5 h, used crude; (f) **9**, SOCl₂, DMA, -5 °C to rt, 3 h, 33%; (g) CsF, TMSCF₃, DMF, rt, 81% for the mixture of diastereomers.

the tetrahydronaphthalene (Table 2). Previously, an agreement docking technique had been used for design of GR agonists.¹² The method was effective but slow and limited by reliance on visual inspection of many docking results. To broaden the use of the method it was automated. A calculated averaged 3D similarity was used as a measure of agreement rather than a simple visual assessment (see the Experimental Section for a description of the technique). This automated agreement docking was applied to the five active R-isomers of the GR binding compounds described in the original work (Figure 2).¹² The automation method performed well and made it possible to explore many more poses than were previously considered. In a fraction of the time used for the manual method it was possible to reproduce the original results, with one interesting exception: it was found that benzoxazine-containing compounds in Figure 2 were now clearly placed with the benzoxazine ring rotated through 180° relative to the original docking mode (Figures 3 and 4). This new agreement docking model was adopted for all further studies of the benzoxazine derivatives.

It appeared from this model that some substitution at position 1 of the tetrahydronaphthalene moiety would be tolerated and an examination of the region showed that space was available for reasonably large substitution (Figure 5). However, the indication from the modeling work was that while substitution here would be tolerated, it was unlikely to improve binding affinity. The modeling was proved correct in this respect, as the favored enantiomers of R¹ substituted compounds gave similar pIC₅₀'s in the binding assay, each close to 8.1 (see Table 2). However, surprisingly, the R¹ substituent had a profound and subtle effect on GR agonism; subsequently, we came to describe the R¹ group as the "agonist trigger". Interestingly, the R¹ group is shown in the docking model to project into a region between helix 3 (H3) and the H11–H12 loop (Figure 5). Changes in this group could modify the behavior of the H12, which forms part of the AF2 region; the positioning of this helix is known to be key to some agonist activities of nuclear hormones.^{19,20}

Replacement of the R¹ hydrogen with a methyl group provides a substantial increase in potency and efficacy in the NFκB assay, with the most potent enantiomer **35d** (D2E2) being a partial agonist having pIC₅₀ = 7.7 (61%) (Table 2). One enantiomer

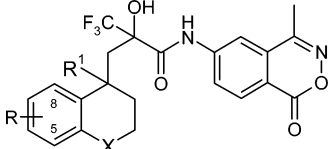
of the other diastereomer **35b** (D1E2) is also a less potent partial agonist having pIC₅₀ = 5.9 (45%). **35d** has little MMTV agonist activity [pIC₅₀ < 5 (4%)] and instead displays micromolar antagonism (pIC₅₀ = 6.4). This compound therefore demonstrates a desired profile with agonism of the transrepression pathway and antagonism of the transactivation pathway as described by these assays in the same A549 cell line. Surprisingly, replacing the R¹ methyl with an ethyl group leads to a further 5-fold increase in agonist potency and increased efficacy, with **36** having NFκB pIC₅₀ = 8.3 (73%). Encouragingly, this compound exhibits weaker efficacy as an MMTV agonist (pIC₅₀ = 8.04 (31%)).

In this series, GR agonism appears balanced on a knife edge; conversion of the tetrahydronaphthalene to the corresponding chromans **37** or **38** leads to a dramatic loss of agonist potency and efficacy with the compounds being GR antagonists. The sensitivity of the 4-position (that is, the R⁴ atom) in the tetrahydronaphthalene toward agonism cannot be explained through modeling studies, which suggest that **36** and **37** bind in an essentially identical fashion with very little difference in possible effects on H12. Furthermore, conformational studies demonstrated that **36** and **37** have essentially the same conformational preferences, eliminating that as a possible cause for the lack of agonism in **37**.

We decided to investigate the effect of aromatic substitution in the tetrahydronaphthalene with GR agonist **36** (R¹ = Et) series. The readily accessible 5-, 6-, and 7-nitro analogues **39**–**41** prove to be excellent binders to GR but lose all agonism, being sub-micromolar antagonists.

The suberan derivative with an R¹ = Et group **42** was also prepared. In contrast to the R¹ = H series, where the suberan derivative **5** is a more potent and efficacious GR agonist than the corresponding tetrahydronaphthalene **4b**, in this series it is less efficacious (compare **36** 73% max with **42** 55% max).

Having **36** in hand with GR agonist potency similar to prednisolone **3**, **36** was evaluated in a mouse DTH in vivo model after topical dosing. This model evaluates the ability of the compound to act as an anti-inflammatory by comparing the thickness of the topically treated right ear with that of the untreated left ear after challenge.¹⁸ Gratifyingly, **36** proved to be an anti-inflammatory agent with an ED₅₀ = 6.5 μg, 10 times

Table 2. Biological Data for Modification of R¹ Substituted Tetrahydronaphthalenes


compd	stereo. ^a	R ⁵⁻⁸	X	R ¹	pIC ₅₀			MMTV ^{b,e} agonism pEC ₅₀ (% max)
					GR binding ^{b,c}	NFκB ^{b,d} (% max)	MMTV ^{b,f} antagonism	
2					8.10 ± 0.04	8.93 ± 0.07 (110 ± 5)	<5	8.3 ± 0.23 (102 ± 10.8)
3					nt ^g	8.07 ± 0.15 (98.4 ± 3.8)	nt	7.50 ± 0.49 (100.3 ± 0.15)
RU486 ^h					8.24 ± 0.09	<6 (4 ± 2)	8.33 ± 0.36	nt
35a	D1E1	–	CH ₂	Me	6.5 ± 0.05	<5 (18 ± 11)	nt	nt
35b	D1E2	–	CH ₂	Me	8.1 ± 0.04	5.9 ± 0.7 (45 ± 13)	nt	nt
35c	D2E1	–	CH ₂	Me	6.6 ± 0.39	<5 (46 ± 4)	nt	nt
35d	D2E2	–	CH ₂	Me	8.0 ± 0.29	7.7 ± 0.32 (61 ± 7)	6.4 ± 0.10	<5 (4 ± 3)
36	D2E1	–	CH ₂	Et	8.21 ± 0.21	8.3 ± 0.43 (73 ± 11)	6.7 ± 0.44	8.04 ± 0.14 (31 ± 9)
37	D2	–	O	Et	7.78 ± 0.01	<5 (46 ± 19)	nt	nt
38	D1	–	O	Et	7.93 ± 0.01	<5 (39 ± 10)	nt	nt
39	D2E1	5-NO ₂	CH ₂	Et	8.3 ± 0.02	<5 (26 ± 10)	6.6 ± 0.07	nt
40	D2E1	6-NO ₂	CH ₂	Et	8.1 ± 0.04	<5 (35 ± 9)	6.1 ± 0.02	nt
41	D2E1	7-NO ₂	CH ₂	Et	8.2 ± 0.19	<5 (19 ± 5)	6.5 ± 0.06	nt
42	D2E1	–	(CH ₂) ₂	Et	8.0 ± 0.03	8.1 ± 0.36 (55 ± 3)	nt	<5 (6 ± 2)

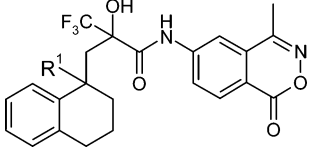
^a D = diastereomer, E = enantiomer. The stereochemistry of the diastereomers has been consistently assigned by retention time on LC/MS. Enantiomer assignment is based on the order of elution from analytical chiral HPLC. See the text for further details. ^b pIC₅₀ values are from duplicate wells with at least *n* = 3 from 11 point dose–response curves with a top concentration of 10 mM. Standard errors are shown. ^c In the GR binding assay, compounds were tested for their ability to bind to GR using competition experiments with fluorescently labeled dexamethasone. ^d The NFκB assay used human A549 lung epithelial cells engineered to contain a secreted placental alkaline phosphatase gene under the control of the distal region of the NFκB dependent ELAM promoter. With a top concentration of 10 mM being tested, pIC₅₀'s are not quoted for values <6. Maxima are quoted with reference to the maximum for dexamethasone (**2**) (the standard used). ^e The MMTV transactivation assay human A549 lung epithelial cells were engineered to contain a renilla luciferase gene under the control of the distal region of the LTR from the mouse mammary tumor virus. ^f The GR antagonist assay used human A549 lung epithelial cells stably transfected with the mouse mammary tumor virus (MMTV) luciferase reporter gene. Compounds were tested for their ability to antagonize dexamethasone-induced activation. ^g nt = not tested. ^h RU486 (mifepristone) was used as the standard for GR antagonism.

less potent than dexamethasone **2** (which correlates approximately with the difference observed in agonist activity) (Table 4).

The ability of the R¹ substituent to trigger GR agonism prompted us to explore this part of the molecule in greater depth. We therefore prepared and tested a range of analogues in order to determine the optimal nature of different alkyl, branched alkyl, cycloalkyl, and phenyl substituents (Table 3). All eleven substituents are potent binders to GR but vary widely in their agonist potency and efficacy in the NFκB assay. For NFκB potency, the SAR for the carbon atom of the R¹ substituent connected to the tetrahydronaphthalene indicates a very clear preference for sp³ geometry over sp² geometry (exemplified by **62**, which is an antagonist), and a general trend of substitutions such as branched chain alkyls and smaller cyclic rings tend to be superior to linear alkyl substitutions that in turn are much superior to highly hindered substitution (exemplified by **59**, which is a micromolar antagonist). Comparison of the propyl or butyl series—normal, iso, or cyclo—suggests that the increases in observed agonist potency is not driven by increases in log *P* but by the impact of molecular structural changes in the binding site. The most potent agonists are the 1-ethylpropyl **52**

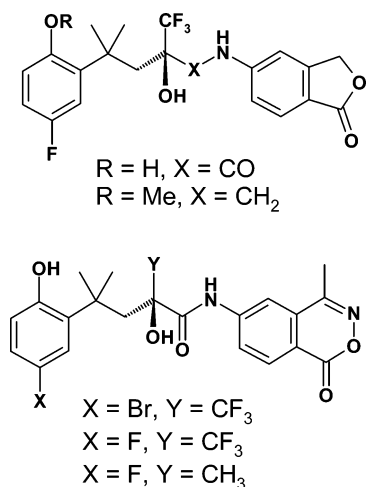
and the cyclopentyl **60** analogues having NFκB pIC₅₀'s of 8.9 (105%) and 8.7 (92%), respectively. Interestingly, in the NFκB assay, a clear trend is observed for this series, where increasing potency (pIC₅₀) correlates with increasing efficacy (% max) (Figure 6).

Various structural modeling studies were carried out in attempts to understand the agonist activities seen for different R¹ groups. Clearly, increasing steric bulk in the region generally improves NFκB agonism. Such a change may be expected to affect the H11–H12 loop. However, all attempts to model the H11–H12 loop movements, in response to changing R¹ groups, were unsuccessful. Molecular dynamics simulations failed to show a significant difference for the position of the loop, at least on the relatively short time scales employed (200 ps). Attempts to understand some of the R¹ groups' SAR were more successful. Two R¹ substituted analogues showed rather surprising activity: the tBu derivative **59** and the phenyl derivative **62**. Both bind well to the GR receptor (see Table 3) but fail to produce agonism. This is in stark contrast to the high potency of close analogues (**55** and **60**). Clearly, placing steric bulk at R¹ is not in itself the key to agonism. The two inactive analogues were docked, using FLO+ (mcdock + 600 cycles),²¹ to the

Table 3. Biological Data for the Modification of the Tetrahydronaphthalene R¹ Substituent


compd	stereo. ^a	R ¹	pIC ₅₀			MMTV ^{b,e} agonism pEC ₅₀ (% max)
			GR binding ^{b,c}	NFκB ^{b,d} (% max)	MMTV ^{b,f} antagonism	
2			8.10 ± 0.04	8.93 ± 0.07 (110 ± 5)	<5	8.3 ± 0.23 (102 ± 10.8)
3			nt ^g	8.07 ± 0.15 (98.4 ± 3.8)	nt	7.50 ± 0.49 (100.3 ± 0.15)
RU486 ^h			8.24 ± 0.09	<6 (4 ± 2)	8.33 ± 0.36	nt
52	D2E2	1-ethylpropyl	8.28 ± 0.03	8.92 ± 0.25 (105 ± 21)	7.18 ± 0.2	8.20 ± 0.22 (47 ± 13)
53	D2E2	nPr	8.25 ± 0.56	8.33 ± 0.15 (81 ± 14)	7.60 ± 0.05	7.7 ± 0.05 (14 ± 2)
54	D2E2	cPr	8.33 ± 0.30	8.02 ± 0.38 (57 ± 8)	6.69 ± 0.10	7.4 ± 0.05 (15 ± 6)
55	D2E2	iPr	8.32 ± 0.21	8.53 ± 0.32 (77 ± 7)	6.89 ± 0.22	7.73 ± 0.05 (43 ± 18)
56	D2E2	nBu	8.51 ± 0.36	8.18 ± 0.24 (65 ± 3)	nt	<6 (7 ± 4)
57	D2E2	iBu	8.46 ± 0.32	7.8 ± 0.47 (50 ± 5)	6.29 ± 0.04	<6 (4 ± 4)
58	D2E2	cBu	8.02 ± 0.14	8.31 ± 0.29 (80 ± 7)	6.78 ± 0.33	7.76 ± 0.08 (27 ± 5)
59	D2E2	tBu	7.94 ± 0.29	<5 (42 ± 10)	6.11 ± 0.53	nt
60	D2E2	cPent	8.09 ± 0.35	8.69 ± 0.45 (92 ± 22)	7.27 ± 0.6	7.75 ± 0.58 (39 ± 9)
61	D2E2	cHex	8.07 ± 0.31	8.48 ± 0.15 (92 ± 8)	6.70 ± 0.21	7.68 ± 0.1 (34 ± 9)
62	D2E2	Ph	7.84 ± 0.27	<5 (45 ± 43)	5.86 ± 0.04	nt

^a D = diastereomer, E = enantiomer. The stereochemistry of the diastereomers has been consistently assigned by retention time on LC/MS. Enantiomer assignment is based on the order of elution from analytical chiral HPLC. See the text for further details. ^b pIC₅₀ values are from duplicate wells with at least $n = 3$ from 11 point dose–response curves with a top concentration of 10 mM. Standard errors are shown. ^c In the GR binding assay, compounds were tested for their ability to bind to GR using competition experiments with fluorescently labeled dexamethasone. ^d The NFκB assay used human A549 lung epithelial cells engineered to contain a secreted placental alkaline phosphatase gene under the control of the distal region of the NFκB dependent ELAM promoter. With a top concentration of 10 mM being tested, pIC₅₀'s are not quoted for values <6. Maxima are quoted with reference to the maximum for dexamethasone (**2**) (the standard used). ^e The MMTV transactivation assay human A549 lung epithelial cells were engineered to contain a renilla luciferase gene under the control of the distal region of the LTR from the mouse mammary tumor virus. ^f The GR antagonist assay used human A549 lung epithelial cells stably transfected with the mouse mammary tumor virus (MMTV) luciferase reporter gene. Compounds were tested for their ability to antagonize dexamethasone-induced activation. ^g nt = not tested. ^h RU486 (mifepristone) was used as the standard for GR antagonism.

**Figure 2.** Structures of analogues used in the “agreement docking method”.

agreement docking protein by applying H-bond tethers to constrain the benzoxazine ring and the central tertiary alcohol

Table 4. ED₅₀'s for **36**, **52**, and **60** in the Topical Mouse Delayed Type Hypersensitivity (DTH)^a

compd	2	36	52	60
ED ₅₀ (μg)	0.27	5, 8 ^b	0.35	0.05, 0.25 ^b
NFκB pIC ₅₀	8.93	8.3	8.9	8.7

^a After sensitization, groups of mice were dosed topically with compound on the right ear. One hour later both ears were challenged with sensitizer, and 3 h postchallenge, the animals were dosed with compound again on the right ear. Twenty-four hours later the thickness of each ear was recorded.¹⁸ ^b Values from two independent experiments.

to the agreement docking mode and allowing the tetrahydronaphthalene and R¹ groups freedom to explore binding modes. Although both **59** and **62** could produce the expected agreement mode, it was found that a very similar but different mode was also favored. In this mode the R¹ group and the tetrahydronaphthalene group were reversed within the site (see Figure 7 for comparison of **60** and **62**). Importantly, similar behavior was not seen with the potent agonist analogues. It is possible that in the living cell, the preferred ligand protein complex for **59** and **62** is this alternative arrangement rather than the previously identified agreement docking and further-

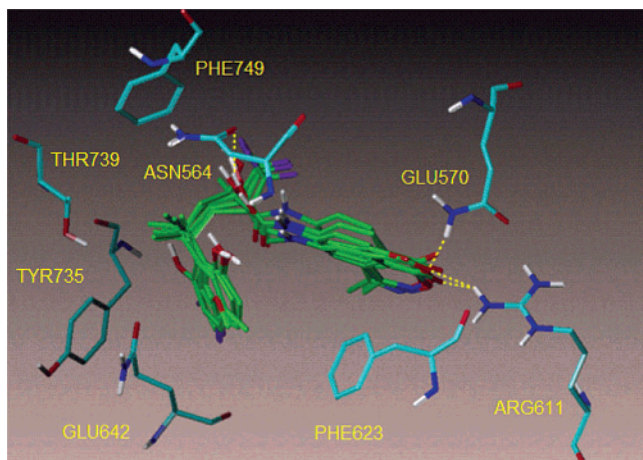


Figure 3. Automated agreement docking showing key protein residues (in cyan) and multiple dockings of the structures from Figure 2 (in green). Hydrogen bonds (dotted yellow lines) between the tertiary alcohols of the ligands and Asn564 are shown together with those between the phthalide or benzoxazine with Glu570 and Arg611.

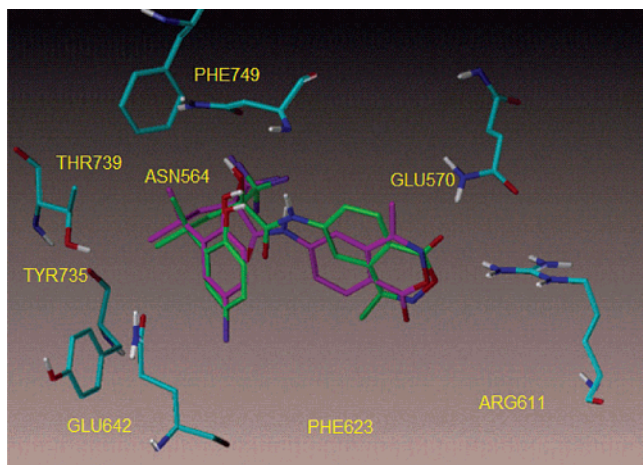


Figure 4. Comparison of automated (green) and manual (purple) docking for one of the benzoxazine ligands from Figure 2. Note the benzoxazine is rotated through 180°.

more that this alternative mode allows binding but fails to provide the subtle agonist trigger. Certainly an examination of this docking mode indicates a diminished likelihood of interaction with the H11–H12 loop.

As described earlier, these R¹ analogues display TR/TA selectivity as judged by their reduced efficacy in the A549 MMTV assay (Table 3). From a plot of the percentage maxima for NFκB vs MMTV (Figure 8), there is a clear trend that NFκB percentage maxima correlate with increasing MMTV percentage maxima. The TR/TA selectivity compared with the standard steroids **2** and **3** is clear; comparing **52** and **2**, which have similar potency and efficacy, **52** is ca. 50% efficacy selective for TR over TA. It may therefore be surmised that this structural series typically demonstrates ca. 50% TR/TA selectivity, with the *n*-propyl analogue **53** having an increased selectivity of ca. 67% and the isopropyl analogue **55** having decreased selectivity of ca. 34%. The partial efficacy of this series of R¹ analogues in the MMTV agonism assay is reflected by their profile as potent antagonists in a dexamethasone-induced activation antagonist assay at sub-micromolar concentrations with the *n*-propyl analogue **53** having a pIC₅₀ of 7.60 (25 nM).

Both **52** and **60** were tested topically in the *in vivo* mouse DTH model, showing 10-fold increased anti-inflammatory

activity when compared with **36** and with approximately equivalent activity to dexamethasone (**2**) (Table 4).

The cyclopentyl **60** and isopentyl **52** analogues were tested against a panel of nuclear receptors including the androgen (AR), estrogen (ER), mineralocorticoid (MR), and progesterone (PR) receptors in binding and functional assays (data not shown). No activity is observed against ER and at least 50-fold selectivity for GR over AR is observed in both binding and functional assays. The compounds show at least 100-fold selectivity for GR (in the NFκB assay) when compared with MR antagonism. The cyclopentyl analogue **60** is equipotent with PR in both binding and agonist assays, whereas the isomeric 1-ethylpropyl analogue **52** shows 10-fold selectivity for GR over PR in both assays.

These data show that by optimization of the R¹ position alone from R¹ = H to 1-ethylpropyl **52** or cyclopentyl **60** converts antagonists (or very partial agonists) into full agonists, increases potency by 3 orders of magnitude, and modulates both TR/TA and nuclear receptor selectivity! The *in vitro* selective TR/TA profiles of this series of compounds hold promise for exploring how such selectivity is manifested *in vivo* in terms of their ability to act as anti-inflammatory agents with a reduced side effect profile.

Experimental Section

Chemistry. General Experimental Conditions. Two LC/MS systems were used. System 1 consisted of a Waters ZQ platform with a HP1050 auto sampler. The column was a 3.3 cm × 4.6 mm 3 μm ABZ+PLUS with a flow rate of 3 mL/min and an injection volume of 5 μL. UV detection was in the range 215–330 nm. The mobile phase consisted of 0.1% formic acid plus 10 mM ammonium acetate (solvent A) and 95% acetonitrile plus 0.05% formic acid (solvent B) with a gradient of 100% A for 0.7 min changing to 100% B over 3.5 min, maintained for 1.1 min and then reverting to 100% A over 0.2 min.

System 2 consisted of a Finnigan TSQ700 platform with electrospray source operating in positive or negative ion mode with a HP1050 autosampler. The column was a 100 × 3 mm 5 μm Higgins Cliepus C18 with a flow rate of 2 mL/min. UV detection was at 254 nm. The mobile phase consisted of water plus 0.1% formic acid (solvent A) and acetonitrile plus 0.1% formic acid (solvent B) with a gradient of 95% A for 1 min changing to 5% A over 14 min, maintained for 2 min, reverted to 95% A over 1 min, and maintained for 2 min. System 1 was used except where stated otherwise.

Mass-directed autopreparation was carried out using a Micromass ZMD platform. The column was a 100 × 20 mm 5 μm Supelco LCABZ++ column with a flow rate of 20 mL/min. The mobile phase consisted of water plus 0.1% formic acid (solvent A) and MeCN:water 95:5 plus 0.05% formic acid (solvent B).

Mass-directed chromatography was carried out on a 10 cm × 21.3 mm 5 μm Supelco column with a flow rate of 20 mL/min. The injection volume was 500 μL and the UV detection range was 200–320 nm. The mobile phase consisted of water plus 0.1% formic acid (solvent A) and 60% MeCN plus 0.05% formic acid (solvent B) with a gradient of 40% A for 1 min changing to 35% A over 9 min and then changing to 1% A over 3.5 min, maintained for 1.4 min before reverting to 40% A over 0.1 min.

Biotage-based chromatography refers to flash chromatography using prepacked silica cartridges on equipment available from Biotage.

¹H NMR spectra were recorded on a Bruker DPX 400 or Inova-400 spectrometer in CDCl₃, CD₃OD, or DMSO-*d*₆ solution. High-resolution mass spectra (HRMS) were determined on a Micromass Q-ToF 2 mass spectrometer by electrospray ionization in positive mode.

Ethyl (2*E*/*Z*)-2-Ethoxy-3-(1,2,3,4-tetrahydronaphthalen-1-yl)prop-2-enoate (7). *n*-Butyllithium (1.6 M in hexanes) (6.6 mL,

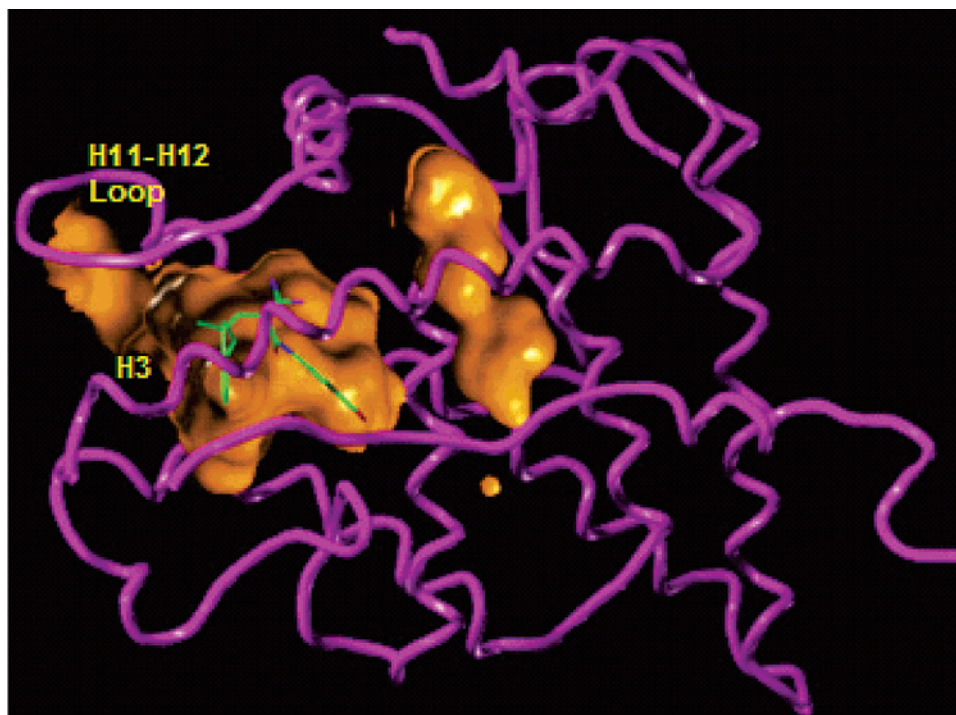


Figure 5. Compound **35b** in the agreement docking mode. The R¹ group can be seen to project into the region between H3 and the H11–H12 loop.

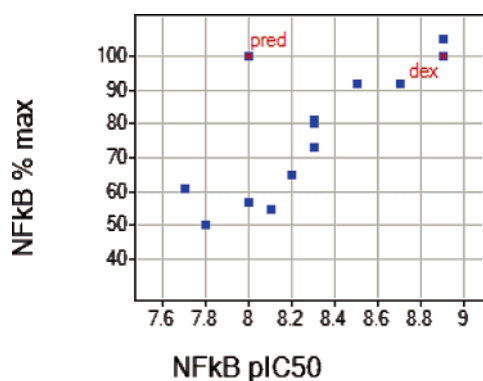


Figure 6. Plot of NFkB % max vs NFkB pIC₅₀ for agonists from Tables 2 and 3. Dexamethasone (**2**) and prednisolone (**3**) are labeled.

10.6 mmol) was added to diisopropylamine (1.49 mL, 10.6 mmol) in THF (15 mL) at -10°C . After 15 min, triethyl phosphonoethoxyacetate (2.86 g, 10.6 mmol) was added followed 30 min later by **6** (1.71 g, 10.6 mmol). The mixture was allowed to warm to room temperature and stirred overnight. After quenching with brine (25 mL) and 2 M HCl (25 mL), the mixture was extracted with EtOAc (2×50 mL). The combined extracts were washed with brine, dried (MgSO_4), and concentrated. Purification by Biotage eluting with 49:1 cyclohexane:Et₂O gave 2.27 g (78%) of **7** as a mixture of *E* and *Z* isomers. LC/MS: $t_{\text{R}} = 3.71, 3.75$ min; $\text{MH}^+ = 275$. ¹H NMR (CDCl_3 , 400 MHz): δ 7.03–7.15 (m, 4H), 6.20–6.25 (d, $J = 9.4$ Hz, 0.25 H), 5.15–5.20 (d, $J = 10.0$ Hz, 0.75H), 4.35–4.15 (m, 2.5H), 4.1–3.85 (m, 1H), 3.8–3.7 (t, $J = 8.2$ Hz, 1.5H), 2.8 (m, 2H), 2.05–1.8 (m, 2H), 1.7–1.5 (m, 2H), 1.35–1.2 (m, 6H).

2-Oxo-3-(1,2,3,4-tetrahydronaphthalen-1-yl)propanoic Acid (8). **7** (1.5 g, 5.5 mmol), trifluoroacetic acid (20 mL), and water (15 mL) were mixed at room temperature for 3 h. The solvents were then removed in vacuo and the residue azeotroped with toluene (3×25 mL) and dried in vacuo overnight to give 1.3 g (quantitative yield) of **8** as a crystalline solid that was used without further purification. LC/MS: $t_{\text{R}} = 3.32\text{--}3.8$ min; $\text{MH}^- = 217$.

***N*-(4-Methyl-1-oxo-1*H*-2,3-benzoxazin-6-yl)-2-oxo-3-(1,2,3,4-tetrahydronaphthalen-1-yl)propanamide (10).** To a solution of **8** (229 mg, 1.05 mmol) in dimethylacetamide (7.3 mL) at -8°C was added thionyl chloride (0.117 mL, 1.6 mmol) in one portion. After raising the temperature to 0°C , **9** (129 mg, 0.73 mmol) was added and the mixture stirred for 3 h, warming to room temperature. After removing the solvents in vacuo, the residue was purified by silica SPE (10 g) eluting with 20-mL fractions of DCM ($\times 6$), CHCl_3 ($\times 4$), and Et₂O ($\times 2$). The desired fractions were combined, concentrated, and triturated with DCM to give 142 mg (52%) of **10** as a white solid. LC/MS: $t_{\text{R}} = 3.6$ min; $\text{MH}^+ = 377$. ¹H NMR (CDCl_3 , 400 MHz): δ 9.25 (s, 1H), 8.45 (d, $J = 7.8$ Hz, 1H), 8.40 (s, 1H), 7.95 (d, $J = 8.9$ Hz, 1H), 7.30–7.10 (m, 4H), 3.62 (m, 1H), 3.55 (m, 2H), 2.96–2.80 (m, 2H), 2.7 (s, 3H), 2.06–1.7 (m, 4H).

3,3,3-Trifluoro-2-hydroxy-*N*-(4-methyl-1-oxo-1*H*-2,3-benzoxazin-6-yl)-2-(1,2,3,4-tetrahydronaphthalen-1-ylmethyl)propanamide (4a, 4b). To a solution of **10** (121 mg, 0.32 mmol) in DMF (5 mL) at room temperature were added trimethylsilyltrifluoromethane (0.248 mL, 1.68 mmol) and cesium carbonate (125 mg, 0.38 mmol). After stirring overnight, TBAF (1.9 mL of a 1 M solution in THF) was added. After 30 min, the mixture was diluted with water (50 mL) and extracted with EtOAc (2×50 mL). The combined extracts were washed with water (100 mL), dried (MgSO_4), and concentrated in vacuo. Purification by Biotage eluting with cyclohexane:EtOAc 4:1 gave 18 mg (26%) of **4a** (diastereomer 1) and 15 mg (21%) of diastereomer 2. LC/MS: $t_{\text{R}} = 3.57$ min (diastereomer 2) and 3.61 min (diastereomer 1); $\text{MH}^+ = 447$, $\text{MH}^- = 445$ (both peaks). HRMS for $\text{C}_{23}\text{H}_{22}\text{F}_3\text{N}_2\text{O}_4$ (MH^+): calcd 447.1532, found 447.1533. ¹H NMR (CDCl_3 , 400 MHz): δ 8.76 (s, 1H), 8.20 (d, $J = 5.3$ Hz, 1H), 8.16 (s, 1H), 7.60 (m, 1H), 7.07 (m, 1H), 6.93 (m, 3H), 2.95 (m, 1H), 2.76–2.58 (m, 3H), 2.48 (s, 3H), 2.16 (dd, $J = 15.1, 8.5$ Hz, 1H), 1.91–1.59 (m, 4H).

Diastereomer 1 was separated into its enantiomers using a 2×25 cm Chiralpak AD column eluting with 10% EtOH in heptane with a flow rate of 15 mL/min. Enantiomer 1 of **4b** eluted after 14.1 min (6.2 mg) and enantiomer 2 eluted after 17.0 min (5.9 mg). Analytical chiral HPLC (25×0.46 cm Chiralpak AD column, 15% 2-propanol in heptane eluting at 1 mL/min): $t_{\text{R}} = 9.20$ min

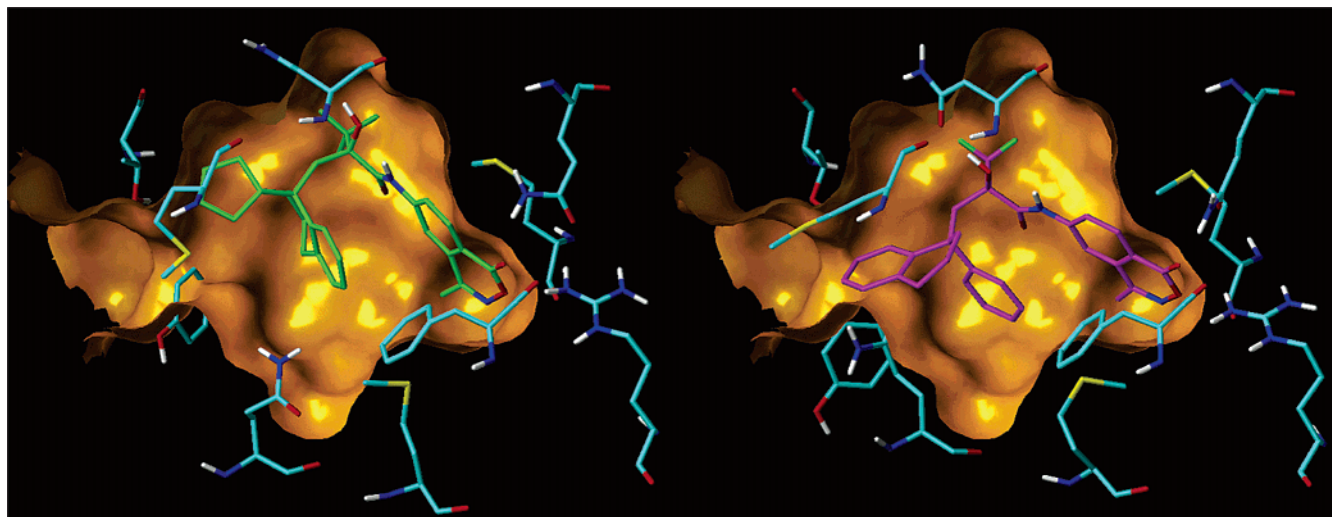


Figure 7. Right: compound **60** in the “agreement docking mode” with the R¹ group oriented upward. Left: compound **62** in a similar but different docking with R¹ group oriented downward.

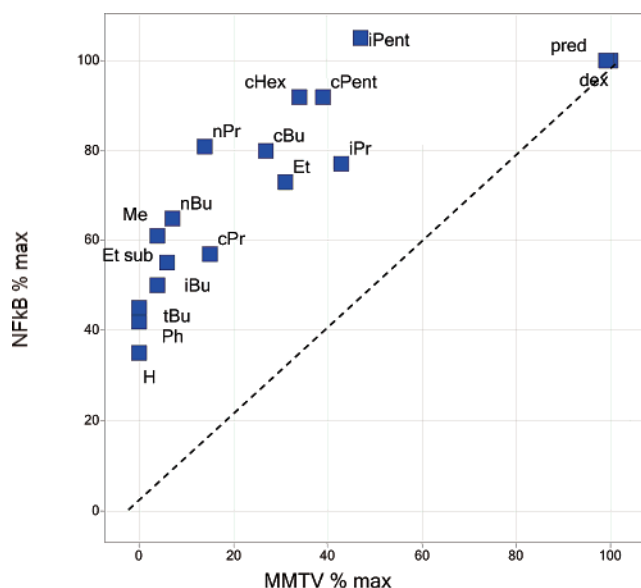


Figure 8. Plot of NfκB % max vs MMTV % max for agonists from Tables 2 and 3. The dotted line represents where nonefficacy selective compounds would lie on the plot. Note the analogues from Table 3 (labeled) are left-shifted with respect to the dotted line illustrating their efficacy selectivity observed with the data from the NfκB and MMTV assays.

(enantiomer 1) and 10.88 min (enantiomer 2). LC/MS: $t_R = 3.57$ min; $MH^+ = 447$, $MH^- = 445$ (both peaks).

3,3,3-Trifluoro-2-[(8-fluoro-1,2,3,4-tetrahydro-1-naphthalenyl)-methyl]-2-hydroxy-N-(4-methyl-1-oxo-1H-2,3-benzoxazin-6-yl)-propanamide (29). Compound **11** (0.145 g, 0.3 mmol), stannous chloride dihydrate (0.44 g, 2 mmol), and THF (2.5 mL) were heated at 60 °C for 3 h. After cooling and concentration in vacuo, purification using an aminopropyl Bond Elut eluting with MeOH followed by a gravity column on SiO₂ eluting with 2.5% MeOH in CHCl₃ gave 0.071 g (49%) of the amino compound. LC/MS: $t_R = 3.37$ min; $MH^+ = 462$, $MH^- = 460$. ¹H NMR (DMSO-*d*₆, 400 MHz): δ 8.48 (m, 1H), 8.35 (m, 1H), 8.25 (d, $J = 7.5$ Hz, 1H), 6.79 (t, $J = 7.5$ Hz, 1H), 6.43 (d, $J = 6.0$ Hz, 1H), 6.28 (d, $J = 7.5$ Hz, 1H), 2.76–2.62 (m, 2H), 2.58 (m, 1H), 2.47 (s, 3H), 2.30 (m, 2H), 2.0 (dd, $J = 15.3, 8.4$, 1H), 1.94–1.82 (m, 1H), 1.68–1.45 (m, 2H).

Boron trifluoride etherate (8 μL, 0.065 mmol) was cooled to –15 °C. The amino compound (0.02 g, 0.0434 mmol) in dry THF (0.1 mL) was added. A solution of *tert*-butyl nitrite (6.2 μL, 0.052 mmol) was added over 10 min and the mixture was left at room

temperature overnight. The mixture was concentrated and the residue was partitioned between water and chloroform. The aqueous layer was further extracted with chloroform, and the combined extracts were dried and evaporated in vacuo. Initial purification by silica SPE followed by preparative TLC gave 2 mg (9.9%) of **29**. LC/MS: $t_R = 3.55$ min; $MH^+ = 465$. ¹H NMR (CDCl₃, 400 MHz): δ 8.47 (s, 1H), 8.43 (d, $J = 6.8$ Hz, 1H), 8.30 (s, 1H), 7.83 (d, $J = 8.6$ Hz, 1H), 7.1 (m, 1H), 6.92 (d, $J = 6.8$ Hz, 1H), 6.80 (m, 1H), 3.42 (m, 1H), 3.20 (m, 2H), 2.83 (m, 1H), 2.75 (m, 1H), 2.60 (s, 3H), 2.47 (dd, $J = 15.4, 8.2$, 1H), 2.35 (m, 1H), 2.25 (m, 1H), 1.83 (m, 1H), 1.70 (m, 1H).

3,3,3-Trifluoro-2,2-dihydroxy-N-(4-methyl-1-oxo-1H-2,3-benzoxazin-6-yl)propanamide (12). Formic acid (20.4 mL) was added dropwise over 5 min to chilled (0 °C) acetic anhydride (41.8 mL). The mixture was warmed to 55 °C and stirred for 2 h. A suspension of **9** (22.0 g, 0.125 mol) in THF (500 mL) under N₂ was prepared. To this was added the first solution. The mixture was stirred under N₂ at room temperature for 72 h, at which point the solvent was removed in vacuo to give 25.7 g (quantitative yield) of the formamido compound as a white solid that was used without further purification. LC/MS: $t_R = 2.17$ min; $MH^+ = 205$.

The formamido compound (12.4 g, 60.8 mmol) was partially dissolved in DMPU (73 mL) and then THF (182 mL) was added to give a suspension. Triethylamine (25.3 mL, 182 mmol) followed by phosphorus oxychloride (6.63 mL, 71.5 mmol) was added, and the mixture was allowed to stir at room temperature under N₂ for 20 h. The solvent was removed in vacuo and the residue was diluted with sodium bicarbonate (500 mL, 5% aqueous solution) and extracted with EtOAc (3 × 500 mL). The organic extracts were combined, washed with water (500 mL), and dried (Na₂SO₄), and the solvent was reduced in vacuo. The residue was triturated using DCM to give 7.97 g of the isonitrile as a pale brown solid. LC/MS: $t_R = 2.37$ min.

The isonitrile (7.58 g) was suspended in trifluoroacetic anhydride (143 mL) and stirred at room temperature for 46 h. The reaction mixture was cooled in an ice bath and quenched with methanol (143 mL) and the solvent/reagent removed in vacuo. The remaining material was azeotroped with toluene. Purification by Si chromatography eluting with cyclohexane:EtOAc (gradient of 2:1 to 1:5) gave 8.2 g (46%) of **12** as an off-white solid. LC/MS: $t_R = 2.53$ min; $MH^+ = 319$, $MNH_4^+ = 336$. ¹H NMR (DMSO-*d*₆, 400 MHz): δ 10.8 (s, 1H), 8.43 (d, 1H), 8.40–8.35 (br d, 3H), 8.24 (d, 1H), 2.5 (s, 3H).

3,3,3-Trifluoro-2-hydroxy-N-(4-methyl-1-oxo-1H-2,3-benzoxazin-6-yl)-2-[5-methoxy-1,2,3,4-tetrahydro-1-naphthalenyl]-methyl]propanamide (17, diastereomer 1 of 16). 5-Methoxy-tetralone (0.5 g, 2.8 mmol) was dissolved in THF (10 mL) and cooled to 0 °C. To this was added μ -chloro- μ -methylene[bis-

(cyclopentadienyl)titanium]dimethylaluminum (Tebbe reagent) (0.5 M in toluene, 5.6 mL, 2.8 mmol), the mixture was allowed to come to room temperature and stirred for 2 h, and then ether (10 mL) was added. The reaction was quenched by the cautious addition of 2 M NaOH solution, filtered, and dried over MgSO₄. Volatiles were removed in vacuo to give an orange oil (1.6 g). Purification by Biotage eluting with DCM gave 0.3 g (61%) of the methylene compound as a yellow oil. ¹H NMR (CDCl₃, 400 MHz): δ 7.34 (m, 1H), 7.19 (m, 1H), 6.77 (d, *J* = 5.7 Hz, 1H), 5.54 (s, 1H), 5.03 (s, 1H), 3.86 (s, 3H), 2.85 (m, 2H), 2.52 (m, 2H), 1.93 (m, 2H).

The methylene compound (143 mg, 0.82 mmol) and **12** (312 mg, 0.98 mmol) were mixed together in a flask and then placed into a preheated (200 °C) oil bath for 10 min and cooled to room temperature. Purification on a 10-g Si SPE cartridge eluting with 4% MeCN/DCM gave 301 mg (77%) of the coupled product. ¹H NMR (CDCl₃, 400 MHz): δ 8.27 (d, *J* = 9.0 Hz, 1H), 8.10 (s, 1H), 7.50 (m, 1H), 7.08 (t, *J* = 7.05 Hz, 1H), 6.90 (d, *J* = 7.05 Hz, 1H), 6.67 (d, *J* = 7.05 Hz, 1H), 6.15 (m, 1H), 3.73 (s, 3H), 3.62 (d, *J* = 15.1 Hz, 1H), 3.12 (d, *J* = 15.1 Hz, 1H), 2.58 (m, 2H), 2.55 (s, 3H), 2.22 (m, 2H). LC/MS: *t*_R = 3.38 min; MH⁻ = 473.

A mixture of the coupled product (100 mg, 0.21 mmol), tosyl hydrazide (78 mg, 0.42 mmol), and NMP (7 drops) was heated at 150 °C for 16 min, during which time further quantities (78 mg) of tosyl hydrazide were added every 4 min. The mixture was cooled and applied directly to a Si SPE cartridge eluted with DCM and 1–3% MeCN/DCM mixtures. The appropriate fractions were combined and evaporated to give a yellow foam that was subjected to mass-directed autopreparation to give 12.4 mg (25%) of **17** (diastereomer 1) and 16.7 mg (33%) of diastereomer 2. LC/MS: *t*_R = 3.56 min (diastereomer 1) and 3.61 min (diastereomer 2); both peaks MH⁺ = 477, MH⁻ = 475. ¹H NMR (CD₃OD, 400 MHz): δ 8.29–8.26 (m, 2H), 8.16 (m, 1H), 6.89 (t, *J* = 7.5 Hz, 1H), 6.79 (d, *J* = 7.5 Hz, 1H), 6.58 (d, *J* = 7.5 Hz, 1H), 3.73 (s, 3H), 2.99 (m, 1H), 2.72–2.61 (m, 2H), 2.55 (s, 3H), 2.50 (m, 1H), 2.08 (dd, *J* = 15, 8.5, Hz 1H), 2.00 (m, 1H), 1.92–1.72 (m, 3H). HRMS for C₂₄H₂₄F₃N₂O₅ (MH⁺): calcd 477.1637, found 477.1628.

3,3,3-Trifluoro-2-hydroxy-*N*-(4-methyl-1-oxo-1*H*-2,3-benzoxazin-6-yl)-2-[(5-nitro-1,2,3,4-tetrahydro-1-naphthalenyl)methyl]propanamide (24). To a suspension of methyltriphenylphosphonium bromide (4.4 g, 12.5 mmol) in THF (50 mL) at –45 °C was added a solution of BuLi (1.6 M in hexanes, 7.3 mL, 11.7 mmol). The resulting dark red suspension was stirred at –45 °C for 1 h and then a solution of 5-nitrotetralone²⁵ (1.5 g, 7.8 mmol) in THF (25 mL) was added over 5 min. The reaction mixture was allowed to come to room temperature and then poured slowly onto water. The aqueous mixture was extracted with cyclohexane, and the combined extracts were dried and evaporated in vacuo. Purification of the residue via Biotage eluting with 2.5% EtOAc/cyclohexane gave 970 mg (66%) of the Wittig product. ¹H NMR (CDCl₃, 400 MHz): δ 7.88 (d, *J* = 7 Hz, 1H), 7.72 (d, *J* = 7 Hz, 1H), 7.29 (t, *J* = 7 Hz, 1H), 5.51 (s, 1H), 5.12 (s, 1H), 3.02 (t, *J* = 7 Hz, 2H), 2.63 (m, 2H), 1.9 (m, 2H).

Further reaction of the Wittig product was similar to that described for **17** to give a mixture of diastereomers. Mass-directed autopreparation separated diastereomer 1 (**24**) as a yellow gum. ¹H NMR (CDCl₃, 400 MHz): δ 9.25 (s, 1H), 8.38 (d, *J* = 8.5 Hz, 1H), 8.33 (d, *J* = 2.0 Hz, 1H), 7.79 (dd, *J* = 8.5, 2.0 Hz, 1H), 7.60 (d, *J* = 8.0 Hz, 1H), 7.53 (d, *J* = 7.5 Hz, 1H), 7.21 (t, *J* = 8.0 Hz, 1H), 5.38 (br s, 1H), 3.12 (m, 1H), 3.02–2.87 (m, 2H), 2.70 (dd, *J* = 14.5, 3.5 Hz, 1H), 2.62 (s, 3H), 2.21 (dd, *J* = 14.5, 9.0 Hz, 1H), 2.03–1.78 (m, 4H). LC/MS: *t*_R = 3.5 min; MH⁺ = 492, MH⁻ = 490. HRMS for C₂₃H₂₁F₃N₃O₆ (MH⁺): calcd 492.1382, found 492.1378.

2-[(5-Amino-1,2,3,4-tetrahydro-1-naphthalenyl)methyl]-3,3,3-trifluoro-2-hydroxy-*N*-(4-methyl-1-oxo-1*H*-2,3-benzoxazin-6-yl)propanamide (22). A mixture of **24** (33 mg, 0.07 mmol), tin(II) chloride (90 mg, 0.4 mmol), and THF (1 mL) was heated at 60 °C for 45 min and then allowed to stir at room temperature overnight. The reaction mixture was diluted with EtOAc and the pH was taken to 6 using sodium bicarbonate solution. Precipitated solids were

filtered off, and the organic layer of the filtrate was separated. The aqueous layer was extracted with EtOAc, and the combined organic solutions were dried and evaporated to a brown oil. Purification by silica SPE eluting with DCM, chloroform, ether, and EtOAc gave 24 mg of **22** (75%) as a yellow solid. LC/MS: *t*_R = 3.04 min; MH⁺ = 462, MH⁻ = 460. ¹H NMR (CD₃OD, 400 MHz): δ 8.26–8.18 (m, 2H), 8.13 (dd, *J* = 8.5, 2.0 Hz, 1H), 6.68 (t, *J* = 7.5 Hz, 1H), 6.59 (d, *J* = 7.5 Hz, 1H), 6.44 (d, *J* = 8.0 Hz, 1H), 2.94 (m, 1H), 2.62 (dd, *J* = 15.0, 5.0 Hz, 1H), 2.56–2.45 (m, 5H), 2.37 (m, 1H), 2.06 (dd, *J* = 15.0, 8.0 Hz, 1H), 2.05–1.88 (m, 2H), 1.86–1.75 (m, 2H). HRMS for C₂₃H₂₃F₃N₃O₄ (MH⁺): calcd 462.1641, found 462.1633.

2-[(5-Bromo-1,2,3,4-tetrahydro-1-naphthalenyl)methyl]-3,3,3-trifluoro-2-hydroxy-*N*-(4-methyl-1-oxo-1*H*-2,3-benzoxazin-6-yl)propanamide (23a–23f) was prepared from 5-bromotetralone similarly to **17** utilizing the Wittig reagent. LC/MS (diastereomer 1, **23a**): *t*_R = 3.78 min, (diastereomer 2, **23b**) *t*_R = 3.85 min; MH⁺ = 525, 527, MH⁻ = 523, 525 (both peaks). **23a**: ¹H NMR (CDCl₃, 400 MHz): δ 8.96 (s, 1H), 8.37 (d, *J* = 8.5 Hz, 1H), 8.29 (d, *J* = 2.0 Hz, 1H), 7.77 (dd, *J* = 8.5, 2.0 Hz, 1H), 7.33 (d, *J* = 7.5 Hz, 1H), 7.17 (d, *J* = 7.5 Hz, 1H), 6.91 (t, *J* = 7.5 Hz, 1H), 3.09 (m, 1H), 2.85 (m, 1H), 2.75–2.65 (m, 2H), 2.62 (s, 3H), 2.26 (dd, *J* = 15.0, 8.0 Hz, 1H), 1.96–1.84 (m, 4H). HRMS for C₂₃H₂₁BrF₃N₂O₄ (MH⁺): calcd 525.0367, found 525.0640. **23b**: ¹H NMR (CDCl₃, 400 MHz): δ 9.16 (s, 1H), 8.40–8.36 (m, 2H), 7.87 (dd, *J* = 8.5, 2.0 Hz, 1H), 7.41 (d, *J* = 7.0 Hz, 1H), 7.17 (d, *J* = 7.5 Hz, 1H), 7.01 (t, 7.5 Hz, 1H), 3.20 (m, 1H), 2.85–2.68 (m, 2H), 2.71 (d, *J* = 9.5 Hz, 1H), 2.64 (s, 3H), 2.24 (dd, *J* = 15.1, 3.5 Hz, 1H), 1.86 (s, 1H), 1.77 (s, 1H), 1.68 (t, *J* = 4.3 Hz, 2H). HRMS for C₂₃H₂₁BrF₃N₂O₄ (MH⁺): calcd 525.0637, found 525.0634.

Compound **23a** was separated into its enantiomers using a 25 cm Chiralcel OD-H column eluting with 15% EtOH in heptane with a flow rate of 15 mL/min. Compound **23c** (enantiomer 1) eluted around 10.6 min and **23d** (enantiomer 2) around 16.0 min.

Analytical chiral HPLC (25 × 0.46 cm Chiralcel OD-H column, 15% EtOH in heptane eluting at 1 mL/min): 11.41 min (enantiomer 1) and 17.83 min (enantiomer 2). LC/MS: *t*_R = 3.78 min; MH⁺ = 525, 527, MH⁻ = 523, 525 (both peaks). Compound **23b** was separated into its enantiomers using a 25 cm Chiralpak AD column eluting with 15% IPA in heptane with a flow rate of 15 mL/min. Compound **23e** (enantiomer 1) eluted around 12.6 min and **23f** (enantiomer 2) around 15.7 min. Analytical chiral HPLC (25 × 0.46 cm Chiralpak AD column, 15% IPA in heptane eluting at 1 mL/min): 9.55 min (enantiomer 1) and 11.80 min (enantiomer 2). LC/MS: *t*_R = 3.85 min; MH⁺ = 525, 527, MH⁻ = 523, 525 (both peaks).

1-Methyl-1,2,3,4-tetrahydronaphthalen-1-ol (31). Cerium chloride (25 g) was suspended in anhydrous THF (100 mL) at 5 °C and then stirred for 1.5 h under nitrogen. The mixture was cooled to –70 °C and methylolithium (64 mL of a 1.6 M solution in Et₂O) was added over 15 min. When addition was complete, the mixture was stirred for 30 min then a solution of α-tetralone (9.85 g) in THF (50 mL) was added over 30 min and stirring at –65 °C was continued for 2 h. The ice bath was removed and the mixture was stirred at room temperature overnight, quenched with 5% acetic acid (100 mL), filtered through Celite, and extracted with EtOAc (400 mL). The aqueous layer was further extracted with EtOAc (2 × 100 mL), and the combined extracts were washed with water (1×) and brine (2×), dried over magnesium sulfate, and evaporated in vacuo to a brown solid (10.32 g). Flash chromatography using cyclohexane:EtOAc 20:1 gave the product **31** as a white solid (5 g). ¹H NMR (CDCl₃, 400 MHz): δ 7.61 (d, *J* = 7.5 Hz, 1H), 7.16–7.07 (m, 2H), 6.90 (d, *J* = 7.5 Hz, 1H), 2.78–2.64 (m, 2H), 1.89–1.69 (m, 5H), 1.48 (s, 3H). LC/MS: *t*_R = 3.62 min; MH⁺ = 163. TLC: SiO₂, 18:2 cyclohexane:EtOAc, *R*_f = 0.22.

Methyl 3-(1-Methyl-1,2,3,4-tetrahydronaphthalen-1-yl)-2-oxopropanoate (32). To **31** (0.73 g) and methyl 2-(trimethylsiloxy)acrylate²⁶ (1.8 g) in CHCl₃ (250 mL) at –60 °C was added tin tetrachloride (1 M in DCM) (3.4 mL) dropwise over 30 s. After 5 min the reaction was quenched with brine (50 mL) and the organic layer separated, dried (MgSO₄), and concentrated in vacuo. This

was purified on 3 × 50 g SPE cartridges eluting with cyclohexane: EtOAc 50:0 to 35:15 in 1 mL increments to yield the title compound **32** (0.196 g). ¹H NMR (CDCl₃, 400 MHz): δ 7.30–7.08 (m, 4H), 3.76 (s, 3H), 3.32 (d, *J* = 15 Hz, 1H), 3.16 (d, *J* = 15 Hz, 1H), 2.91–2.76 (m, 2H), 2.07–1.99 (m, 1H), 1.95–1.67 (m, 3H), 1.47 (s, 3H). TLC: SiO₂, 12:3 cyclohexane:EtOAc, *R*_f = 0.29.

3-(1-Methyl-1,2,3,4-tetrahydronaphthalen-1-yl)-2-oxopropanoic Acid 33. **32** (0.196 g) was dissolved in methanol (28 mL). To this was added solid potassium hydroxide (0.18 g) and the mixture was stirred at room temperature for 2 h. Volatiles were removed in vacuo, and the residue was diluted with water and then washed with Et₂O. The aqueous phase was acidified with 2 M HCl and extracted with DCM. The combined extracts were dried and evaporated to yield the title compound **33** as a gum (0.176 g). ¹H NMR (CDCl₃, 400 MHz): δ 7.32–7.05 (m, 4H), 3.50 (d, *J* = 15.5 Hz, 1H), 3.28 (d, *J* = 15.5 Hz, 1H), 2.95–2.78 (m, 2H), 2.10–2.00 (m, 1H), 1.95–1.65 (m, 3H), 1.45 (s, 3H). LC/MS: *t*_R = 3.68 min; MH⁺ = 231.

N-(4-Methyl-1-oxo-1H-2,3-benzoxazin-6-yl)-3-(1-methyl-1,2,3,4-tetrahydronaphthalen-1-yl)-2-oxopropanamide (34). **33** (0.156 g) was azeotroped three times from toluene and then dissolved in dimethylacetamide (5.5 mL) at –5 °C under nitrogen. To this was added thionyl chloride (74 μL) and after 10 min the temperature was raised to +5 °C. After 20 min 6-amino-4-methyl-2,3-benzoxazin-1-one **9** (0.108 g) was added and the mixture was stirred for 3 h at room temperature. Volatiles were removed in vacuo, and the residue was purified by silica SPE (10 g) eluting with 20 mL fractions of DCM (×4), Et₂O (×4) and EtOAc (×4). The desired fractions were combined and concentrated to afford the title compound **34** as a white foam (0.178 g). ¹H NMR (CDCl₃, 400 MHz): δ 9.05 (s, 1H), 8.34 (d, *J* = 8.57 Hz, 1H), 8.22 (s, 1H), 7.78 (m, 1H), 7.28 (m, 1H), 7.15–7.05 (m, 3H), 3.52 (d, *J* = 15.7 Hz, 1H), 3.38 (d, *J* = 15.7 Hz, 1H), 2.90–2.75 (m, 2H), 2.57 (s, 3H), 2.13–2.03 (m, 1H), 1.95–1.67 (m, 3H), 1.45 (s, 3H). LC/MS: *t*_R = 3.62 min; MH⁺ = 391.

3,3,3-Trifluoro-2-hydroxy-N-(4-methyl-1-oxo-1H-2,3-benzoxazin-6-yl)-2-[(1-methyl-1,2,3,4-tetrahydronaphthalen-1-yl)methyl]propanamide (35a–35d). **34** (0.15 g) was dissolved in dry DMF (9.7 mL) and cooled to 0 °C. To this were added trimethylsilyltrifluoromethane (0.286 mL) and cesium carbonate (0.158 g). After stirring at room temperature for 3 h, TBAF (1.92 mL of a 1 M solution in THF) was added. After 30 min the mixture was acidified with 1 M HCl (6.4 mL) and extracted with EtOAc. The combined extracts were washed with brine, dried, and concentrated in vacuo to a gum (0.27 g). Purification by flash chromatography eluting with cyclohexane:EtOAc 7:3 followed by mass-directed chromatography gave the following.

Diastereomer 1 (2.0 mg): ¹H NMR (CDCl₃, 400 MHz): δ 8.48 (s, 1H), 8.32 (d, *J* = 8.5 Hz, 1H), 8.14 (s, 1H), 7.51 (dd, *J* = 8.5, 2.0 Hz, 1H), 7.00–6.90 (m, 3H), 3.36 (bs, 1H), 2.95 (d, *J* = 15.1 Hz, 1H), 2.75 (m, 2H), 2.60 (s, 3H), 2.32 (d, *J* = 15.1 Hz, 1H), 2.12–2.03 (m, 1H), 1.90 (m, 1H), 1.77–1.68 (m, 2H), 1.43 (s, 3H). LC/MS: *t*_R = 3.54 min; MH⁺ = 461, MH[–] = 459.

Diastereomer 2 (2.4 mg): ¹H NMR (CDCl₃, 400 MHz): δ 9.00 (s, 1H), 8.38–8.33 (m, 2H), 7.73–7.67 (m, 1H), 7.42 (d, *J* = 7.5 Hz, 1H), 7.32–7.15 (m, 2H), 2.92 (d, *J* = 15.6 Hz, 1H), 2.83–2.69 (m, 4H), 2.61 (s, 3H), 1.84–1.65 (m, 4H), 1.36 (s, 3H). LC/MS: *t*_R = 3.62 min; MH⁺ = 461, MH[–] = 459.

Diastereomer 1 (4.1 mg) was separated into its enantiomers using a 2 × 25 cm Chiralpak AD column eluting with 10% EtOH in heptane with a flow rate of 15 mL/min. **35a** (D1E1) eluted after 9.2 min (1.0 mg) and **35b** (D1E2) after 13.4 min (1.1 mg). **35a**: Analytical chiral HPLC (25 × 0.46 cm Chiralpak AD column, 10% EtOH in heptane eluting at 1 mL/min): 7.42 min. LC/MS: *t*_R = 3.54 min; MH⁺ = 461, MH[–] = 459. **35b**: Analytical chiral HPLC (25 × 0.46 cm Chiralpak AD column, 10% EtOH in heptane eluting at 1 mL/min): 11.17 min. LC/MS: *t*_R = 3.54 min; MH⁺ = 461, MH[–] = 459.

Diastereomer 2 (2.5 mg) was separated into its enantiomers using a 2 × 25 cm Chiralpak AD column eluting with 10% EtOH in heptane with a flow rate of 15 mL/min. **35c** (D2E1) eluted after

11.0 min (0.82 mg) and **35b** (D2E2) after 14.4 min (0.92 mg). **35c**: Analytical chiral HPLC (25 × 0.46 cm Chiralpak AD column, 10% EtOH in heptane eluting at 1 mL/min): 9.12 min. LC/MS: *t*_R = 3.62 min; MH⁺ = 461, MH[–] = 459. **35d**: Analytical chiral HPLC (25 × 0.46 cm Chiralpak AD column, 10% EtOH in heptane eluting at 1 mL/min): 11.78 min. LC/MS: *t*_R = 3.62 min; MH⁺ = 461, MH[–] = 459.

3,3,3-Trifluoro-2-hydroxy-N-(4-methyl-1-oxo-1H-2,3-benzoxazin-6-yl)-2-[(1-ethyl-1,2,3,4-tetrahydronaphthalen-1-yl)methyl]propanamide (D2E1) (36). **N**-(4-Methyl-1-oxo-1H-2,3-benzoxazin-6-yl)-3-(1-ethyl-1, 2,3,4-tetrahydronaphthalen-1-yl)-2-oxopropanamide (prepared similarly to **34**) (0.57 g) was dissolved in dry DMF (9 mL). To this was added trimethylsilyltrifluoromethane (1 g) and cesium carbonate (0.55 g). The mixture was stirred at room temperature for 1 h, after which time further trimethylsilyltrifluoromethane (0.4 g) was added and stirring at room temperature was continued overnight. Volatiles were removed in vacuo, and the residue was partitioned between water and DCM. The organic layer was dried and applied directly to a 50-g Si SPE cartridge eluted with DCM and DCM:MeCN 10:1. Evaporation of the appropriate fractions in vacuo gave a mixture of diastereomers (0.32 g). This was purified by reverse phase preparative HPLC using a 45–80% MeCN (0.05% TFA) gradient over 50 min on a Supelcosil ABZ+ 10 cm × 21.2 mm column with a 4 mL/min flow rate. This gave the following.

Diastereomer 1 (110 mg): ¹H NMR (CDCl₃, 400 MHz): δ 8.36 (s, 1H), 8.30 (d, *J* = 8.5 Hz, 1H), 8.11 (d, *J* = 2.0 Hz, 1H), 7.45 (dd, *J* = 8.5, 2.0 Hz, 1H), 7.21 (m, 1H), 6.99 (m, 1H), 6.93–6.85 (m, 2H), 3.31 (bs, 1H), 2.91 (d, *J* = 15.1 Hz, 1H), 2.76–2.73 (m, 2H), 2.60 (s, 3H), 2.31 (d, *J* = 15.1 Hz, 1H), 1.96–1.86 (m, 4H), 1.78–1.70 (m, 2H), 0.82 (t, *J* = 7.5 Hz, 3H). LC/MS: *t*_R = 3.64 min; MH⁺ = 475, MH[–] = 473.

Diastereomer 2 (107 mg): ¹H NMR (CDCl₃, 400 MHz): δ 9.00 (s, 1H), 8.36 (d, *J* = 8.5 Hz, 1H), 8.32 (d, *J* = 2.0 Hz, 1H), 7.70 (dd, *J* = 8.5, 2.3 Hz, 1H), 7.38 (d, *J* = 7.8 Hz, 1H), 7.31–7.17 (m, 2H), 2.99 (d, *J* = 15.3 Hz, 1H), 2.81 (s, 1H), 2.79–2.74 (m, 2H), 2.65 (d, *J* = 15.3 Hz, 1H), 2.61 (s, 3H), 1.90–1.51 (m, 6H), 0.90 (t, *J* = 7.5 Hz, 3H). LC/MS: *t*_R = 3.72 min; MH⁺ = 475, MH[–] = 473.

Diastereomer 2 (107 mg) was separated into its enantiomers using a 2 × 25 cm Chiralpak AS column eluting with 10% EtOH in heptane with a flow rate of 15 mL/min. **36** (D2E1) eluted after 11.56 min (30 mg) and **D2E2** eluted after 14.63 min (26 mg).

36 (D2E1): Analytical chiral HPLC (25 × 0.46 cm Chiralpak AS column, 10% EtOH in heptane eluting at 1 mL/min): 9.07 min. LC/MS: *t*_R = 3.72 min; MH⁺ = 475, MH[–] = 473. HRMS for C₂₅H₂₆F₃N₂O₄ (MH⁺): calcd 475.1845, found 475.1841. CD (MeCN, rt ν = 350–190 nM): 203.0 nM (de = –10.42; *E* = 23 414), 210.0 nM (de = –9.52; *E* = 16 706), 243.0 nM (de = 10.35; *E* = 29 387), 281.4 nM (de = 4.51; *E* = 14 213).

D2E2: Analytical chiral HPLC (25 × 0.46 cm Chiralpak AS column, 10% EtOH in heptane eluting at 1 mL/min): 11.29 min. LC/MS: *t*_R = 3.72 min; MH⁺ = 475, MH[–] = 473.

3,3,3-Trifluoro-2-hydroxy-N-(4-methyl-1-oxo-1H-2,3-benzoxazin-6-yl)-2-[(1-ethyl-5-nitro-1,2,3,4-tetrahydronaphthalen-1-yl)methyl]propanamide (39), 3,3,3-Trifluoro-2-hydroxy-N-(4-methyl-1-oxo-1H-2,3-benzoxazin-6-yl)-2-[(1-ethyl-6-nitro-1,2,3,4-tetrahydronaphthalen-1-yl)methyl]propanamide (40), and 3,3,3-Trifluoro-2-hydroxy-N-(4-methyl-1-oxo-1H-2,3-benzoxazin-6-yl)-2-[(1-ethyl-7-nitro-1,2,3,4-tetrahydronaphthalen-1-yl)methyl]propanamide (41). K₁₀ montmorillonite clay (3.26 g) was added to a stirred suspension of copper(II) nitrate hydrate (2.952 g, 12.7 mmol) in acetone (40 mL). The reaction was stirred for 10 min and then concentrated in vacuo to give a light blue solid. This solid was powdered and further dried in vacuo to afford the clay–copper complex. Loading was calculated as 2.04 mmol/g.

Acetic anhydride (0.3 mL, 3.18 mmol) was added to a stirred solution of **36** (15 mg, 0.0316 mmol) in dichloromethane (0.3 mL) under nitrogen atmosphere. The clay–copper complex (25 mg, 0.0506 mmol) was added and the reaction was stirred at room temperature for 16 h. The reaction was diluted with dichloromethane

(2 mL) and filtered through a pad of Celite. The filtrate was washed with saturated sodium bicarbonate and extracted with dichloromethane. The combined extracts were washed with brine, dried (PTFE frit), and concentrated to give a yellow oil. Chromatography (silica gel, 1 g, 3:1 cyclohexane:ethyl acetate) gave pure 7-nitro isomer **41** (2.7 mg, 16%) as a white solid and the 5- and 6-nitro isomers **39** and **40** as a mixture (4.1 mg, 25%). The 5-nitro **39** and 6-nitro **40** analogues were separated by reverse phase HPLC (Luna Phenyl Hexyl column, 10 μ M, 150 \times 4.6 mM i.d. with a gradient of 0.1% TFA/H₂O to 0.05% TFA/MeOH with a mass detector set at $m/z = 520$).

39 (5-nitro analogue): ¹H NMR (CDCl₃, 400 MHz): δ 8.39 (s, 1H), 8.38 (d, $J = 8.6$ Hz, 1H), 8.27 (d, $J = 2.2$ Hz, 1H), 7.77 (dd, $J = 8.5, 2.2$ Hz, 1H), 7.65–7.62 (m, 2H), 7.41 (t, $J = 7.0$ Hz, 1H), 3.08 (d, $J = 16.0$ Hz, 1H), 2.92–2.85 (m, 2H), 2.62–2.56 (m, 4H), 2.35 (s, 1H), 1.93–1.58 (m, 6H), 0.91 (t, $J = 8.1$ Hz). LC/MS: $t_R = 3.57$ min; $MH^+ = 520$, $MH^- = 518$. HRMS for C₂₅H₂₅F₃N₃O₆ (MH⁺): calcd 520.1695, found 520.1693.

40 (6-nitro analogue): ¹H NMR (CDCl₃, 400 MHz): δ 8.86 (s, 1H), 8.37 (d, $J = 7.8$ Hz, 1H), 8.28 (s, 1H), 8.09–8.02 (m, 2H), 7.71 (dd, $J = 8.3, 1.6$ Hz, 1H), 7.53 (d, $J = 7.53$ Hz, 1H), 3.09 (d, $J = 15.6$ Hz, 1H), 2.90 (m, 2H), 2.66–2.59 (m, 4H), 2.36–2.28 (m, 2H), 1.93–1.75 (m, 3H), 1.68–1.60 (m, 2H), 0.91 (t, $J = 7.8$ Hz). LC/MS: $t_R = 3.56$ min; $MH^+ = 520$, $MH^- = 518$. HRMS for C₂₅H₂₅F₃N₃O₆ (MH⁺): calcd 520.1695, found 520.1695.

41 (7-nitro analogue): ¹H NMR (CDCl₃, 400 MHz): δ 8.82 (brs, 1H), 8.31 (d, 8.5 Hz, 1H), 8.30 (d, $J = 2.0$ Hz, 1H), 8.06 (d, $J = 2.0$ Hz, 1H), 7.83 (dd, $J = 8.5, 2.0$ Hz, 1H), 7.68 (dd, $J = 8.5, 2.0$ Hz, 1H), 7.23 (d, $J = 8.5$ Hz, 1H), 3.05 (d, $J = 15.5$ Hz, 1H), 2.91–2.86 (m, 3H), 2.58 (s, 3H), 2.43 (d, $J = 15.5$ Hz, 1H), 2.02–1.81 (m, 4H), 1.81–1.63 (m, 2H), 0.87 (t, $J = 7.5$ Hz, 3H). LC/MS: $t_R = 3.54$ min; $MH^+ = 520$, $MH^- = 518$. HRMS for C₂₅H₂₅F₃N₃O₆ (MH⁺): calcd 520.1695, found 520.1690.

2-[(5-Ethyl-6,7,8,9-tetrahydro-5H-benzocyclohepten-5-yl)-methyl]-3,3,3-trifluoro-2-hydroxy-N-(4-methyl-1-oxo-1H-2,3-benzoxazin-6-yl)propanamide (D2E1) (42). To 3-(5-ethyl-6,7,8,9-tetrahydro-5H-benzocyclohepten-5-yl)-N-(4-methyl-1-oxo-1H-2,3-benzoxazin-6-yl)-2-oxopropanamide (0.94 g) (prepared similarly to **34**) in dry DMF (15 mL) were added cesium carbonate (0.87 g) and trifluoromethyltrimethylsilane (0.66 mL). After 3 h, further trifluoromethyltrimethylsilane (0.66 mL) was added, and after 18 h, further trifluoromethyltrimethylsilane (0.5 mL) and cesium carbonate (0.56 g) were added. After 5 h, the mixture was added to water (100 mL) and the solid filtered off. The filtrate was extracted with CHCl₃ (2 \times 50 mL), filtered through a Teflon frit, and concentrated in vacuo. Chromatography on silica eluting with CHCl₃ with 1–2% MeOH removed unreacted starting material. To the remainder of the material was added THF (10 mL) and TBAF (1 M in THF) (3 mL). After 45 min, the mixture was added to 1.3 M HCl (100 mL) and CHCl₃ (25 mL). The organic layer was separated using a Teflon frit, concentrated in vacuo, and purified on a silica column eluting with 7:3 40–60 petrol:EtOAc to afford the following.

Diastereomer 1 (58 mg): ¹H NMR (DMSO-*d*₆, 400 MHz): δ 10.55 (s, 1H), 8.24–8.13 (m, 3H), 7.32 (d, $J = 8.0$ Hz, 1H), 7.08 (t, $J = 8.0$ Hz, 1H), 6.85 (t, $J = 7.2$ Hz, 1H), 6.71 (d, $J = 8.0$ Hz, 1H), 3.00 (t, $J = 11.8$ Hz, 1H), 2.67 (d, $J = 14.6$ Hz, 1H), 2.30–2.39 (m, 4H), 2.28 (m, 1H), 2.13 (d, $J = 14.6$ Hz, 1H), 2.05 (m, 1H), 1.89–1.76 (m, 2H), 1.69 (bs, 2H), 1.49–1.39 (m, 2H), 0.76 (t, $J = 7.2$ Hz, 3H). LC/MS: $t_R = 3.77$ min; $MH^+ = 489$.

Diastereomer 2 (43 mg): ¹H NMR (DMSO-*d*₆, 400 MHz): δ 10.16 (s, 1H), 8.10 (d, $J = 8.5$ Hz, 1H), 8.00 (d, $J = 8.5$ Hz, 1H), 7.96 (s, 1H), 7.35 (s, 1H), 7.11 (d, $J = 7.7$ Hz, 1H), 6.88 (d, $J = 6.8$ Hz, 1H), 6.67–6.58 (m, 2H), 3.12–3.01 (m, 2H), 2.78–2.61 (m, 2H), 2.45 (s, 3H), 1.89–1.47 (m, 6H), 1.38–1.07 (m, 2H), 0.79 (t, $J = 7.3$ Hz, 3H). LC/MS: $t_R = 3.77$ min; $MH^+ = 489$.

Diastereomer 2 was separated into its enantiomers using 2 \times 25 cm Chiralpak AS column eluting with 15% EtOH in heptane with a flow rate of 15 mL/min. **42** D2E1 eluted around 7 min and D2E2 eluted around 12 min. **42** D2E1: Analytical chiral HPLC (25 \times 0.46 cm Chiralpak AS column eluting with 15% EtOH in heptane

with a flow rate of 1 mL/min): 5.59 min. LC/MS: $t_R = 3.77$ min; $MH^+ = 489$. HRMS for C₂₆H₂₈N₂O₄F₃ (MH⁺): calcd 489.2001, found 489.2000. **42** D2E2: Analytical chiral HPLC (25 \times 0.46 cm Chiralpak AS column eluting with 15% EtOH in heptane with a flow rate of 1 mL/min): 8.10 min. LC/MS: $t_R = 3.77$ min; $MH^+ = 489$.

5-Ethyl-1-(2-iodophenyl)-4-heptanone (46). Tetrakis(triphenylphosphine)palladium (0.29 g, 0.25 mmol) was cooled to 0 °C and a solution of 1-ethylpropylzinc bromide (0.5 M in THF, 50 mL, 25 mmol) was added. Acryloyl chloride (2.2 mL, 27.1 mmol) was added slowly to keep the temperature below 5 °C, and the mixture was then stirred at 0 °C for 1.5 h. Dried lithium chloride (2.12 g, 50 mmol) and copper(I) cyanide (2.24 g, 25 mmol) in dry THF were stirred for 10 min and then cooled to –75 °C. A solution of benzyl zinc bromide (0.5 M in THF, 50 mL, 25 mmol) was added slowly to maintain the temperature below –67 °C. The resulting mixture was allowed to warm to 0 °C, stirred for 20 min, and then again cooled to –75 °C before the slow addition of chlorotrimethylsilane (6.4 mL, 50.4 mmol) with the temperature kept below –70 °C. The solution of the vinyl ketone prepared above was added slowly below –68 °C. After the addition the mixture was stirred at –75 °C for 2.5 h then allowed to come to room temperature, stirred at this temperature for 2 h, and then partitioned between diethyl ether and water. The aqueous phase was extracted with ether, and the combined organic solutions were washed with brine twice, dried (Na₂SO₄), and evaporated in vacuo to an oil. Purification was by silica chromatography using hexane and hexane: ether 10:1 to give the title compound **46** (3.12 g, 36%). ¹H NMR: (CDCl₃, 400 MHz): δ 7.84 (d, 1H), 7.25 (m, 2H), 6.90 (t, 1H), 2.72 (t, 2H), 2.50 (t, 2H), 2.34 (m, 1H), 1.88 (m, 2H), 1.61 (m, 2H), 1.48 (m, 2H), 0.86 (t, 6H). LCMS: $t_R = 3.87$ min; 345 (MH⁺); 362 (MNH₄)⁺.

1-[4-(1-Ethylpropyl)-4-penten-1-yl]-2-iodobenzene (47). A stirred suspension of methyltriphenylphosphonium bromide (75.6 g, 0.21 mol) in dry THF (600 mL) was stirred at 0 °C while a 1.6 M solution of *n*-BuLi in hexane (120 mL, 0.19 mol) was added slowly below 5 °C. The mixture was stirred at 0 °C for 30 min and then a solution of **46** (30.1 g, 87.5 mmol) in THF (75 mL) was added slowly below 0 °C. After stirring for 15 min, the mixture was stirred at room temperature for 1 h, refluxed overnight, and then cooled to 10 °C. Saturated ammonium chloride solution (250 mL) was added while the temperature was maintained at ca. 10 °C and the mixture was stirred for 15 min and then diluted with water (250 mL). After stirring for a further 15 min the mixture was extracted with diethyl ether. The combined ether extracts were washed with 1:1 saturated ammonium chloride solution:brine (500 mL) and then dried (Na₂SO₄) and evaporated in vacuo. The residue was triturated with hexane and filtered. The filtrate was applied to a column of silica and eluted with hexane to give the title compound **47** (22.5 g, 76%). ¹H NMR: (CDCl₃, 400 MHz): δ 7.78 (d, 1H), 7.50 (m, 2H), 6.90 (t, 1H), 4.88 (s, 1H), 4.77 (s, 1H), 2.73 (t, 2H), 2.03 (t, 2H), 1.80 (m, 3H), 1.40 (m, 4H), 0.83 (t, 6H).

2-[1-(1-Ethylpropyl)-1,2,3,4-tetrahydro-1-naphthalenyl]-1-(2-furanyl)ethanone (48). To palladium acetate (68 mg, 2.92 mmol) and triphenyl phosphine (1.53 g, 5.84 mmol) were added toluene (225 mL) and (2-furyl)tributylstannane (6.78 g, 19 mmol). A solution of **47** (5 g, 14.6 mmol) in toluene (75 mL) was then added and the apparatus was purged three times with carbon monoxide. The mixture was then placed in a preheated 110 °C oil bath and stirred for 3 h under carbon monoxide, diluted with ether (300 mL), and washed with 2 M HCl (300 mL) and with water (300 mL). The organic layer was separated, poured into a solution of KF (40 g) in water (600 mL), stirred for 0.5 h, and then filtered. The organic layer was separated, washed with water (300 mL), dried, and evaporated in vacuo. The preparation was repeated using a further 7.5 g (21.9 mmol) of **47**, and the crude products were combined. Purification was by Biotage chromatography. The solvent gradients used were cyclohexane:DCM 1:0 to 0:1 followed by DCM:EtOAc 3:1 to 0:1, which gave the title compound **48** (2.19 g, 20%). ¹H NMR (CDCl₃, 400 MHz): δ 7.25 (d, 1H), 6.96 (m, 3H), 6.77 (m, 1H), 6.33 (m, 1H), 3.28 (d, 1H), 3.04 (d, 1H), 2.69 (m, 2H), 1.97

(m, 1H), 1.78 (m, 5H), 1.28 (m, 1H), 1.09 (m, 5H), 0.78 (t, 3H). LCMS: t_R 3.95 min; 311 (MH)⁺.

3-[1-(1-Ethylpropyl)-1,2,3,4-tetrahydro-1-naphthalenyl]-2-oxopropanoic Acid (49). Ozone was bubbled through a solution of **48** (2.19 g, 7.1 mmol) in anhydrous methanol (200 mL) at -78 °C for 1 h followed by oxygen for 10 min and nitrogen for 10 min. Dimethyl sulfide (15 mL, 205 mmol) was added and the mixture was stirred for 1 h at room temperature and then evaporated in vacuo. The residue was dissolved in methanol (200 mL), KOH pellets (3 g) were added, and the solution stirred for 1.5 h. Volatiles were removed in vacuo and the residue was partitioned between 2 M KOH solution (300 mL) and a 1:1 mixture of cyclohexane and diethyl ether (300 mL). The aqueous phase was acidified and extracted with DCM (300 mL). The extract was dried (MgSO₄) and evaporated to give the title compound **49** (2.01 g, 99%), which was used without further purification. ¹H NMR (CDCl₃, 400 MHz): δ 7.22 (d, 1H), 7.05 (m, 3H), 3.38 (d, 1H), 3.30 (d, 1H), 2.70 (m, 2H), 2.0–1.61 (m, 6H), 1.31 (m, 1H), 1.15–0.98 (m, 5H), 0.72 (t, 3H).

3-[1-(1-Ethylpropyl)-1,2,3,4-tetrahydro-1-naphthalenyl]-N-(4-methyl-1-oxo-1H-2,3-benzoxazin-6-yl)-2-oxopropanamide (51). **49** (333 mg, 1.15 mmol) was dried by azeotroping from toluene (3 × 5 mL) and the dried material was dissolved in DMA (2.9 mL) and then cooled to -10 °C. Thionyl chloride (243 mg, 2.08 mmol) was added and stirring at -10 °C was continued for 1 h. A solution of 6-amino-4-methyl-1H-2,3-benzoxazin-1-one (407 mg, 2.31 mmol) in DMA (9.5 mL) was added at -6 °C and the mixture was allowed to come to room temperature. After stirring at this temperature for 3 h, the reaction mixture was poured into a 1:1 DCM:2 M HCl mixture. The aqueous layer was extracted with DCM and the combined extracts were dried (MgSO₄) and evaporated in vacuo, and the residue was triturated with DCM. Filtration and evaporation of the filtrate gave a brown oil. Purification was by silica SPE. The solvent gradient used was cyclohexane:EtOAc 20:1 to 0:1 to give the title compound **51** (69 mg, 33%) as yellow crystals. ¹H NMR (CDCl₃, 400 MHz): δ 8.85 (br, 1H), 8.31 (d, 1H), 8.12 (d, 1H), 7.70 (d, 1H), 7.26 (d, 1H), 7.05 (m, 3H), 3.52 (d, 1H), 3.35 (d, 1H), 2.82 (m, 2H), 2.56 (s, 3H), 2.0–1.68 (m, 6H), 1.32 (m, 1H), 1.12 (m, 5H), 0.78 (t, 3H). LCMS: t_R 3.94 min; 464 (M + 18)⁺, 445 (MH)⁻.

3,3,3-Trifluoro-2-hydroxy-N-(4-methyl-1-oxo-1H-2,3-benzoxazin-6-yl)-2-[(1-propyl-1,2,3,4-tetrahydronaphthalen-1-yl)methyl]propanamide (53) (D2E2). 2-Oxo-3-(1-propyl-1,2,3,4-tetrahydronaphthalen-1-yl)propanoic acid (similarly prepared to **51**) (175 mg, 418 μmol) was dissolved in anhydrous DMF (2.5 mL), and dried cesium carbonate (286 mg, 878 μmol) was added in one portion. The reaction mixture was cooled in an ice bath and Me₃SiCF₃ (309 μL, 2.09 mmol) was added. The ice bath was then removed. After approximately 2 h of stirring at 25 °C under nitrogen, the reaction was again cooled in an ice bath and a second portion of Me₃SiCF₃ (124 μL) was added. The reaction was allowed to warm to 25 °C and stirred until TLC (cyclohexane:20% ether) indicated there was no starting material remaining. TBAF (1 M solution in THF, 1 mL) was added to the reaction mixture and the reaction was stirred at 25 °C for 30 min. The mixture was then poured into 1:1:1 brine:saturated ammonium chloride:2 M HCl (10 mL) and extracted with ether (2 × 30 mL). The combined organic extracts were dried on magnesium sulfate, and the solvent was evaporated. The reaction product was purified by chromatography on silica, eluting with cyclohexanes-ethyl acetate 4:1 to give the title compound as a mixture of two diastereoisomers. This mixture of diastereoisomers was purified by reverse phase preparative HPLC using a 45–80% MeCN (0.05% TFA) gradient over 50 min on a Supelcosil ABZ+ 10 cm × 21.2 mm column with a 4 mL/min flow rate. The purification gave the following.

Diastereomer 1 (12.6 mg, 7%): ¹H NMR (CDCl₃, 400 MHz): δ 8.33 (br s, 1H), 8.31 (d, *J* = 8.5 Hz, 1H), 8.12 (d, *J* = 1.8 Hz, 1H), 7.45 (dd, *J* = 8.7, 2.0 Hz, 1H), 7.22 (br d, *J* = 7.1 Hz, 1H), 7.00 (br d, *J* = 6.5 Hz, 1H), 6.93–6.85 (m, 2H), 3.18 (br s, 1H), 2.93 (d, *J* = 15.3 Hz, 1H), 2.75 (br t, *J* = 6.5 Hz, 2H), 2.60 (s, 3H), 2.32 (d, *J* = 15.6 Hz, 1H), 2.02–1.62 (m, 6H), 1.41–1.26

(m, 1H), 1.21–1.09 (m, 1H), 0.85 (t, *J* = 7.3 Hz, 3H). LC/MS: t_R = 3.77 min; (MNH₄)⁺ = 506, MH⁻ = 487.

Diastereomer 2 (8.5 mg, 5%): ¹H NMR (CDCl₃, 400 MHz): δ 8.99 (br s, 1H), 8.36 (d, *J* = 8.6 Hz, 1H), 8.32 (d, *J* = 2.0 Hz, 1H), 7.69 (dd, *J* = 8.8, 2.0 Hz, 1H), 7.39 (d, *J* = 7.8 Hz, 1H), 7.33–7.27 (m, 1H), 7.24–7.15 (m, 2H), 3.01 (d, *J* = 15.4 Hz, 1H), 2.80–2.71 (m, 2H), 2.79 (s, 1H), 2.69 (d, *J* = 15.3 Hz, 1H), 2.61 (s, 3H), 1.90–1.25 (m, 8H), 0.88 (t, *J* = 7.0 Hz, 3H). LC/MS: t_R 3.86 min; MH⁺ = 489, (MNH₄)⁺ = 506, MH⁻ = 487.

Diastereomer 2 was separated into its enantiomers using a 25 cm Chiralpak AD column eluting with 5% EtOH in heptane with a flow rate of 15 mL/min. D2E1 eluted around 17.5 min and D2E2 **53** eluted around 22.5 min. D2E1: Analytical chiral HPLC (25 × 0.46 cm Chiralpak AD column, 5% EtOH in heptane eluting at 1 mL/min): 17.5 min. LC/MS: t_R 3.84 min; (MNH₄)⁺ = 506, (M - H)⁻ = 487. D2E2 **53**: Analytical chiral HPLC (25 × 0.46 cm Chiralpak AD column, 5% EtOH in heptane eluting at 1 mL/min): 21.2 min. LC/MS: t_R = 3.84 min; (MNH₄)⁺ = 506, (M - H)⁻ = 487.

2-[[1-(1-Ethylpropyl)-1,2,3,4-tetrahydro-1-naphthalenyl]methyl]-3,3,3-trifluoro-2-hydroxy-N-(4-methyl-1-oxo-1H-2,3-benzoxazin-6-yl)propanamide (52) (D2E2). Cesium fluoride (130 mg, 856 μmol) was dried at 120 °C for 2 h under vacuum. To this was added a solution of (±) *N*-(4-methyl-1-oxo-1H-2,3-benzoxazin-6-yl)-2-oxo-3-(1-ethylpropyl-1,2,3,4-tetrahydronaphthalen-1-yl)propanamide **51** (77 mg, 172 μmol) in DMF (2 mL) followed by trimethyl(trifluoromethyl)silane (274 μL, 1.85 mmol). The mixture was stirred at room temperature overnight, diluted with DCM (20 mL), and washed with 2 M HCl (10 mL). The aqueous phase was extracted with DCM, and the combined organic solutions were dried (MgSO₄) and evaporated in vacuo. Purification (20 g silica SPE, solvent gradient of cyclohexane:EtOAc 9:1 to 0:1) gave (in order of elution) diastereomer 2 (35.1 mg) and diastereomer 1 (34.3 mg).

Diastereomer 1: ¹H NMR (CDCl₃, 400 MHz): δ 8.27 (d, *J* = 8.5 Hz, 1H), 8.07 (d, *J* = 2.0 Hz, 2H), 7.34 (dd, *J* = 8.6, 2.0 Hz, 1H), 7.27–7.24 (m, *J* = 7.8, 1.3 Hz, 1H), 6.98–6.94 (m, *J* = 7.2, 1.1 Hz, 1H), 6.80–6.71 (m, 2H), 3.18 (s, 1H), 2.92 (d, *J* = 15.0 Hz, 1H), 2.78–2.68 (m, 2H), 2.59 (s, 3H), 2.47 (d, *J* = 15.0 Hz, 1H), 2.05–1.76 (m, 5H), 1.60–1.52 (m, 1H), 1.37–1.25 (m, 2H), 1.10 (t, *J* = 7.5 Hz, 3H), 1.04–0.95 (m, 2H), 0.68 (t, *J* = 7.5 Hz, 3H). LCMS: t_R 3.86 min; 534 (M + 18)⁺, 515 (MH)⁻.

Diastereomer 2: ¹H NMR (CDCl₃, 400 MHz): δ 8.96 (s, 1H), 8.35 (d, *J* = 8.5 Hz, 1H), 8.30 (d, *J* = 2.0 Hz, 1H), 7.69 (dd, *J* = 8.5, 2.0 Hz, 1H), 7.44 (d, *J* = 8 Hz, 1H), 7.30 (m, 1H), 7.26–7.17 (m, 2H), 3.15 (d, *J* = 15.5 Hz, 1H), 2.78 (s, 1H), 2.67–2.74 (m, 2H), 2.61 (s, 3H), 2.57 (d, *J* = 15.5 Hz, 1H), 1.84–1.70 (m, 3H), 1.63 (m, 1H), 1.22–1.33 (m, 2H), 1.02–1.08 (m, 2H), 0.99 (t, *J* = 7.5 Hz, 3H), 0.71 (t, *J* = 7.5 Hz, 3H). LCMS: t_R 3.98 min; 534 (M + 18)⁺, 515 (MH)⁻.

Diastereomer 2 was separated into its enantiomers using a 2 × 25 Chiralpak AD column eluting with 10% EtOH in heptane with a flow rate of 15 mL/min. D2E1 eluted around 7.16 min and **52** D2E2 eluted around 8.41 min.

D2E1: Analytical chiral HPLC (25 × 0.46 cm Chiralpak AD column, 10% EtOH in heptane eluting at 1 mL/min): 5.59 min. LCMS: t_R 3.98 min; 534 (MNH₄)⁺, 515 (MH)⁻. CD (0.000329 M, cell length = 0.1 cm), 210.0 nM (de = 8.51; *E* = 16 886), 243.0 nM (de = -12.78; *E* = 28 070), 277.0 nM (de = -6.09; *E* = 12 828). **52** D2E2: Analytical chiral HPLC (25 × 0.46 cm Chiralpak AD column, 10% EtOH in heptane eluting at 1 mL/min): 6.54 min. LCMS: t_R = 3.98 min; (MNH₄)⁺ = 534, MH⁻ = 515. HRMS for C₂₈H₃₂F₃N₂O₄ (MH⁺): calcd 517.2314, found 517.2311. CD (0.00038 M, cell length = 0.1 cm): 212.0 nM (de = -8.54; *E* = 17 206), 242.6 nM (de = 13.45; *E* = 28 860), 277.0 nM (de = 6.27; *E* = 13 074).

2-[(1-Cyclopentyl)-1,2,3,4-tetrahydro-1-naphthalenyl]methyl]-3,3,3-trifluoro-2-hydroxy-N-(4-methyl-1-oxo-1H-2,3-benzoxazin-6-yl)propanamide (60) (D2E2). Cesium fluoride (99 mg, 652 μmol) was dried in a round-bottomed flask for 2 h under vacuum. The flask was filled with nitrogen and cooled to room temperature. (±)-*N*-(4-Methyl-1-oxo-1H-2,3-benzoxazin-6-yl)-2-oxo-3-(1-cyclo-

pentyl-1,2,3,4-tetrahydronaphthalen-1-yl)propanamide (similarly prepared to **51**) (58 mg, 120 μ mol) in DMF (2 mL) was then added followed by TMSCF₃ (207 μ L, 1.4 mmol) and the mixture was stirred at room temperature overnight. The reaction mixture was concentrated under vacuum, diluted with DCM (20 mL), and washed with 2 M HCl (10 mL). The aqueous phase was extracted with DCM (20 mL) and the organic extract was dried over magnesium sulfate and then evaporated under vacuum to give the crude product. Purification (20 g silica SPE, gradient of cyclohexane:EtOAc 9:1 to 8:2) gave (in order of elution) diastereomer 2 (19.1 mg) and diastereomer 1 (18.8 mg).

Diastereomer 1: ¹H NMR (CDCl₃, 400 MHz): δ 8.27 (d, *J* = 8.5 Hz, 1H), 8.12 (br s, 1H), 8.01 (d, *J* = 2.0 Hz, 1H), 7.34 (dd, *J* = 8.5, 2.0 Hz, 1H), 7.31–7.27 (m, 1H), 6.96–6.91 (m, 1H), 6.88–6.76 (m, 2H), 3.23 (br s, 1H), 2.98 (d, *J* = 15.5 Hz, 1H), 2.76–2.70 (m, 2H), 2.47–2.35 (m, 1H), 2.35 (d, *J* = 15.5 Hz, 1H), 1.97–1.73 (m, 4H), 1.70–1.36 (m, 5H), 1.32–1.18 (m, 2H), 1.08 (s, 1H). LCMS: *t*_R 3.91 min; 532 (M + 18)⁺, 513 (MH)⁻.

Diastereomer 2: ¹H NMR (CDCl₃, 400 MHz): δ 8.98 (s, 1H), 8.35 (d, *J* = 8.5 Hz, 1H), 8.31 (d, *J* = 2.0 Hz, 1H), 7.69 (dd, *J* = 8.5, 2.0 Hz, 1H), 7.44 (d, *J* = 8.0 Hz, 1H), 7.23–7.15 (m, 2H), 2.98 (d, *J* = 15.5 Hz, 1H), 2.82 (s, 1H), 2.79–2.72 (m, 3H), 2.61 (s, 3H), 2.17 (m, 1H), 1.90–1.76 (m, 2H), 1.72–1.62 (m, 4H), 1.60–1.42 (m, 4H), 1.36 (m, 1H), 1.25 (m, 1H). LCMS: *t*_R 4.03 min; 532 (M + 18)⁺, 513 (MH)⁻.

Diastereomer 2 was separated into its enantiomers using a 2 × 25 cm Chiralpak AD column eluting with 5% EtOH in heptane with a flow rate of 15 mL/min. D2E1 eluted around 19.7 min (0.3 mg) and D2E2 **60** eluted around 22.2 min (0.4 mg). D2E1: Analytical chiral HPLC (25 × 0.46 cm Chiralpak AD column, 5% EtOH in heptane eluting at 1 mL/min): 14.2 min. LCMS: *t*_R 4.03 min; 515 (MH)⁺; 532 (MNH₄)⁺; 513 (MH)⁻. CD (0.000 187 M, cell length = 0.2 cm): 211.6 nM (de = 14.32; *E* = 16039), 243.0 nM (de = -13.57; *E* = 29 638), 281.0 nM (de = -5.70; *E* = 13 150). D2E2 **60**: LCMS: *t*_R 4.02 min; 515 (MH)⁺, 532 (MNH₄)⁺, 513 (MH)⁻. HRMS for C₂₈H₃₀N₂O₄F₃ (MH)⁺: calcd 515.2158, found 515.2156. CD (0.000 173 M, cell length = 0.2 cm): 211.4 nM (de = -13.99; *E* = 15 811), 243.2 nM (de = 13.85; *E* = 29 182), 280.8 nM (de = 5.64; *E* = 13 071).

GR Binding Assay. Details of the GR binding assay using a kit supplied by Pan Vera (Madison, WI) are described elsewhere.¹²

Glucocorticoid-Mediated Transrepression of NF κ B Activity. Details of the NK κ B assay are described elsewhere.¹²

Glucocorticoid-Mediated Transactivation of MMTV Driven Gene Expression. Human A549 lung epithelial cells were engineered to contain a renilla luciferase gene under the control of the distal region of the LTR from the mouse mammary tumor virus as previously described.¹⁷ Compounds were solvated and diluted in DMSO and transferred directly into assay plates such that the final concentration of DMSO was 0.7%. Following the addition of cells (40K per well), plates were incubated for 6 h. Luciferase activity was determined using the Firelight kit (Packard, Pangbourne, UK).

Glucocorticoid Antagonist Assay. Details of the MMTV GR antagonist assay are described elsewhere.¹⁷

Oxazolone-Induced Mouse Ear Skin Delayed Type Hypersensitivity Model (DTH). The topical anti-inflammatory activity of the compounds was examined in the Balb/c mouse delayed type hypersensitivity (DTH) model.¹⁸ Inflammation was induced with sensitization to oxazolone (50 μ L of a 25 mg/mL solution, 1 part olive oil to 4 parts acetone) applied topically to the shaved flank of the mouse (female Balb/c, 10–14 g, Charles River, UK). Six animals were used per for each dose. Five days later ear thickness was measured with a pair of engineers' callipers (RS). The animals were then dosed topically with compound on the right ear only (10 μ L volume, ethanol vehicle). One hour later they were challenged with 2.5 mg/mL oxazolone solution (20 μ L volume, 1 part olive oil to 4 parts acetone vehicle) applied topically onto each ear. Three hours postchallenge the animals were dosed with compound again on the right ear only (10 μ L volume, ethanol

vehicle). Twenty-four hours later the ears were remeasured and the thickness recorded. The animals were culled via cervical dislocation.

Automated Agreement Docking. Docking was carried out using form A from the crystal structure of the fluticasone propionate GR complex²⁰ and ligand R isomers only. FLO+ (version Feb03)²¹ was used, applying the mcdock+ technique for 3000 cycles and collecting 25 dockings for each compound. Flexibility of side chains within the site was allowed during the minimization stage of the docking. The docked ligands were extracted from the protein complexes using the FLO+ facility "ligext". These were converted to an SD file using FLO+ facility "mm2sd". The SD structure file was imported into the TSAR package.²² Single-point MNDO calculations were performed within TSAR to assign ESP charges. 3D electrostatic and steric similarities were then calculated between each ligand pair and stored in an *N* × *N* matrix within TSAR. The similarity calculations within TSAR use the methodologies of Good et al.^{23,24} The similarity matrix was then processed using the "auto_agreement_dock" algorithm. This method is a simple genetic algorithm written specifically to search out the combinations of dockings (one from each ligand) that provide the highest overall pairwise similarity. From a random selection of dockings it identifies a reasonable start point and then rapidly mutates the individual dockings, using simple mutations and the averaged pairwise similarity as a fitness function to decide if the mutation should be accepted or not. A Monte Carlo factor can be introduced here to allow some decrease in the averaged similarity during a search for a better solution. The method stores solutions in decreasing order of averaged similarity. The top scoring solution provides the "agreement docking" collection of docked compounds.

Acknowledgment. The authors thank Dr. George W. Hardy and Dr. Keith B. Biggadike for their comments and critical reading of this paper.

Supporting Information Available: Experimental and spectroscopic data for various analogues. This material is available free of charge via the Internet at <http://pubs.acs.org>.

References

- Schimmer, B. P.; Parker, K. L. Adrenocorticotrophic Hormone; Adrenocortical Steroids and Their Synthetic Analogues: Inhibitors of the Synthesis and Actions of Adrenocortical Hormones. In *Goodman & Gilman's The Pharmacological Basis of Therapeutics*, 10th ed; Hardman, J. G., Limbird, L. E., Gilman, A. G., Eds.; McGraw-Hill: New York, 2001; pp1649–1677.
- Buttgereit, F.; Straub, R. H.; Wehling, M.; Burmester, G.-R. Glucocorticoids in the Treatment of Rheumatic Disease. *Arthritis Rheumatism* **2004**, *50*, 3408–3417.
- Schacke, H.; Docke, W. D.; Asdullah, K. Mechanisms Involved in the Side Effects of Glucocorticoids. *Pharm. Ther.* **2002**, *96*, 23–43.
- Resche-Rigon, M.; Gronemeyer, H. Therapeutic Potential of Selective Modulators of Nuclear Receptor Action. *Curr. Opin. Chem. Biol.* **1998**, *2*, 501–507. Barnes, P. J. Anti-Inflammatory Actions of Glucocorticoids: Molecular Mechanisms. *Clin. Sci.* **1998**, *94*, 557–572. Buckbinder, L.; Robinson, R. P. The Glucocorticoid Receptor: Molecular Mechanism and New Therapeutic Opportunities. *Curr. Drug Targets—Inflamm Allergy* **2002**, *1*, 127–36.
- (Abbott/Ligand) Elmore, S. W.; Coghlan, M. J.; Anderson, D. D.; Pratt, J. K.; Green, B. E.; Wang, A. X.; Stashko, M. A.; Lin, C. W.; Tyree, C. M.; Miner, J. N.; Jacobson, P. B.; Wilcox, D. M.; Lane, B. C. Nonsteroidal Selective Glucocorticoid Modulators: The Effect of C-5 Alkyl Substitution on the Transcriptional Activation/Repression Profile of 2,5-Dihydro-10-methoxy-2,2,4-trimethyl-1H-[1]benzopyrano[3,4-*f*]quinolines. *J. Med. Chem.* **2001**, *44*, 4481–4491. Kym, P. R.; Kort, M. E.; Coghlan, M. J.; Moore, J. L.; Tang, R.; Ratajczyk, J. D.; Larson, D. P.; Elmore, S. W.; Pratt, J. K.; Stashko, M. A.; Falls, H. D.; Lin, C. W.; Nakane, M.; Miller, L.; Tyree, C. M.; Miner, J. N.; Jacobson, P. B.; Wilcox, D. M.; Nguyen, P.; Lane, B. C. Nonsteroidal Selective Glucocorticoid Modulators: The Effect of C-10 Substitution on Receptor Selectivity and Functional Potency of 5-Allyl-2,5-dihydro-2,2,4-trimethyl-1H-[1]benzopyrano[3,4-*f*]quinolines. *J. Med. Chem.* **2003**, *46*, 1016–1030 and references therein. Elmore, S. W.; Pratt, J. K.; Coghlan, M. J.; Mao, Y.; Green, B. E.; Anderson, D. D.; Stashko, M. A.; Lin, C. W.; Falls, D.; Nakane,

- M.; Miller, L.; Tyree, C. M.; Miner, J. N.; Lane, B. Differentiation of In Vitro Transcriptional Repression and Activation Profiles of Selective Glucocorticoid Modulators. *Bioorg Med. Chem. Lett.* **2004**, *14*, 1721–1727.
- (6) (Schering) Schacke H.; Schottelius A.; Docke W.-D.; Strehlke P.; Jaroch S.; Schmees N.; Rehwinkel H.; Hennekes H.; Asadullah K. Dissociation of Transactivation from Transrepression by a Selective Glucocorticoid Receptor Agonist Leads to Separation of Therapeutic Effects from Side Effects. *Proc. Nat. Acad. Sci.* **2004**, *101*, 227–32.
- (7) (Merck) Ali, A.; Thompson, C. F.; Balkovec, J. M.; Graham, D. W.; Hammond, M. L.; Quraishi, N.; Tata, J. R.; Einstein, M.; Ge, L.; Harris, G.; Kelly, T. M.; Mazur, P.; Pandit, S.; Santoro, J.; Sitlani, A.; Wang, C.; Williamson, J.; Miller, D. K.; Thompson, C. M.; Zaller, D. M.; Forrest, M. J.; Carballo-Jane, E.; Luell, S. Novel *N*-Arylpyrazolo[3,2-*c*]-Based Ligands for the Glucocorticoid Receptor: Receptor Binding and in Vivo Activity. *J. Med. Chem.* **2004**, *47*, 2441–2452; Thompson, C. F.; Quraishi, N.; Ali, A.; Tata, J. R.; Hammond, M. L.; Balkovec, J. M.; Einstein, M.; Ge, L.; Harris, G.; Kelly, T. M.; Mazur, P.; Pandit, S.; Santoro, J.; Sitlani, A.; Wang, C.; Williamson, J.; Miller, D. K.; Yamin, T. D.; Thompson, C. M.; O'Neill, E. A.; Zaller, D.; Forrest, M. J.; Carballo-Jane, E.; Luell, S. Novel Heterocyclic Glucocorticoids: In Vitro Profile and in Vivo Efficacy. *Bioorg. Med. Chem. Lett.* **2005**, *15*, 2163–2167; Smith, C. J.; Ali, A.; Balkovec, J. M.; Graham, D. W.; Hammond, M. L.; Patel, G. F.; Rouen, G. P.; Smith, S. K.; Tata, J. R.; Einstein, M.; Ge, L.; Harris, G. S.; Kelly, T. M.; Mazur, P.; Thompson, C. M.; Wang, C. F.; Williamson, J. M.; Miller, D. M.; Pandit, S.; Santoro, J. C.; Sitlani, A.; Yamin, T. D.; O'Neill, E. A.; Zaller, D. M.; Carballo-Jane, E.; Forrest, M. J.; Luell, S. Novel Ketal Ligands for the Glucocorticoid Receptor: In Vitro and in Vivo Activity *Bioorg. Med. Chem. Lett.* **2005**, *15*, 2926–2931.
- (8) (Boehringer Ingelheim) Betageri, R.; Zhang, Y.; Zindell, R. M.; Kuzmich, D.; Kirrane, T. M.; Bentzien, J.; Cardozo, M.; Capolino, A. J.; Fadra, T. N.; Nelson, R. M.; Paw, Z.; Shih, D.-T.; Shih, C.-K.; Zuvella-Jelaska, L.; Nabozny, G.; Thomson, D. S. Trifluoromethyl Group as a Pharmacophore: Effect of Replacing a CF₃ Group on Binding and Agonist Activity of a Glucocorticoid Receptor Ligand. *Bioorg. Med. Chem. Lett.* **2005**, *15*, 4761–4769. Marshall, D. R. 3-Sulfonamidoethylindole Derivatives for Use as Glucocorticoid Mimetics in the Treatment of Inflammatory, Allergic and Proliferative Diseases. PCT Int. Appl. 2004, WO 019935. Other patents: WO 059899, 082280, 082787, 101932, 104195 (2003); WO 018429, 063163, 075864 (2004).
- (9) Shah, N.; Scanlan, T. S. Design and Evaluation of Novel Nonsteroidal Dissociating Glucocorticoid Receptor Ligands *Bioorg. Med. Chem. Lett.* **2004**, *14*, 5199–5203.
- (10) Kauppi, B.; Jakob, C.; Farnegardh, M.; Yang, J.; Ahola, H.; Alarcon, M.; Calles, K.; Engstrom, O.; Harlan, J.; Muchmore, S.; Ramqvist, A.-K.; Thorell, S.; Ohman, L.; Greer, J.; Gustafsson, J.-A.; Carlstedt-Duke, J.; Carlquist, M. The Three-dimensional Structures of Antagonistic and Agonistic Forms of the Glucocorticoid Receptor Ligand-Binding Domain. *J. Biol. Chem.* **2003**, 22748–22754. Link, J. T.; Sorensen, B. K.; Lai, C.; Wang, J.; Fung, S.; Deng, D.; Emery, M.; Carroll, S.; Grynfarb, M.; Goos-Nilsson, A.; von Geldern, T. Synthesis, Activity, Metabolic Stability and Pharmacokinetics of Glucocorticoid Receptor Modulator-Statins Hybrids. *Bioorg. Med. Chem. Lett.* **2004**, *14*, 4173–4178 and references therein.
- (11) Morgan, B. P.; Liu, K. K.-C.; Dalvie, D. K.; Swick, A. G.; Hargrove, D. M.; Wilson, T. C.; LaFlamme, J. A.; Moynihan, M. S.; Rushing, M. A.; Woodworth, G. F.; Li, J.; Trilles, R. V.; Yang, X.; Harper, K. W.; Carroll, R. S.; Martin, K. A.; Nardone, N. A.; O'Donnell, J. P.; Faletto, M. B.; Vage, C.; Soliman, V. Discovery of Potent, Non-Steroid and Highly Selective Glucocorticoid Receptor Antagonists with Anti-Obesity Activity. *lett. Drug Des. Discovery* **2004**, *1*, 1–5.
- (12) Barker, M.; Clackers, M.; Demaine, D. A.; Humphreys, D.; Johnston, M. J.; Jones, H. T.; Pacquet, F.; Pritchard, J. M.; Shanahan, S. E.; Skone, P. A.; Vinader, V. M.; Uings, I.; McLay, I. M.; Macdonald, S. J. F. Design and Synthesis of New Non-Steroid Glucocorticoid Modulators through Application of an “Agreement Docking” Method. *J. Med. Chem.* **2005**, *48*, 4507–4510.
- (13) Barker, M. D.; Demaine, D. A.; House, D.; Inglis, G. G. A.; Johnston, M. J.; Jones, H. T.; Macdonald, S. J. F.; McLay, I. M.; Shanahan, S.; Skone, P. A.; Vinader, M. V. Preparation of Heterocycle-Substituted *N*-Benzoxazinylopropanamides as Glucocorticoid Receptor Binders and Agonists for the Treatment of Inflammatory, Allergic and Skin Diseases. PCT Int. Appl. 2004, WO 071389.
- (14) Lehmann, M.; Schollkopf, K.; Strehlke, P.; Heinrich, N.; Fritzemeyer, K.; Muhn, H.; Krattenmacher, R. Non-Steroid (Hetero)cyclically Substituted Acylanilides with Mixed Gestagenic and Androgenic Activity. PCT Int. Appl. 1998, WO 9854159.
- (15) Brown, S.; Clarkson, S.; Grigg, R.; Thomas, W. A.; Sridharan, V.; Wilson, D. M. Palladium Catalyzed Queuing Processes. Part 1: Termolecular Cyclization—Anion Capture Employing Carbon Monoxide as a Relay Switch and Hydride, Organotin(IV) or Boron Reagents. *Tetrahedron* **2001**, *57*, 1347–1359.
- (16) Zhu, L.; Wehmeyer, R. M.; Rieke, R. D. The Direct Formation of Functionalized Alkyl(aryl)zinc Halides by Oxidative Addition of Highly Reactive Zinc with Organic Halides and Their Reactions with Acid Chlorides, α,β -Unsaturated Ketones, and Allylic, Aryl, and Vinyl Halides. *J. Org. Chem.* **1991**, *56*, 1445–53.
- (17) Austin, R. H.; Maschera, B.; Walker, A.; Fairbairn, L.; Meldrum, E.; Farrow, S.; Uings, I. J. Mometasone Furoate is a Less Specific Glucocorticoid Than Fluticasone Propionate. *Eur. Resp. J.* **2002**, *20*, 1386–1392.
- (18) Zhang, L.; Tinkle, S. Chemical Activation of Innate and Specific Immunity in Contact Dermatitis. *J. Invest. Dermatol.* **2000**, *115*, 168–176.
- (19) Brzozowski, A. M.; Pike, A. C.; Dauter, Z.; Hubbard, R. E.; Bonn, T.; Engstrom, O.; Ohman, L.; Greene, G. L.; Gustafsson, J. A.; Carlquist, M. Molecular Basis of Agonism and Antagonism in the Oestrogen Receptor. *Nature* **1997**, *389*, 753–8.
- (20) Bledsoe, R. K.; Lambert, M. H.; Montana, V. G.; Stewart, E. L.; Xu, E. H. Structure of a Glucocorticoid Receptor Ligand Binding Domain Comprising an Expanded Binding Pocket, and Methods Using Nuclear Receptors Structure for Drug Design. *Eur. Pat. Appl.* 1375517, 2004.
- (21) FLO+ (version Feb02, mcdock+ facility) Colin McMartin, Thistle-soft, P.O. Box 227, Colebrook, CT 06021.
- (22) Tsar 3.3 Software, Accelrys Inc.
- (23) Good, A. C.; Hodgkin, E. E.; Richards, W. G. Utilization of Gaussian Functions for the Rapid Evaluation of Molecular Similarity. *J. Chem. Inform. Comput. Sci.* **1992**, *32*, 188–91.
- (24) Good, A. C.; Richards, W. G. Rapid Evaluation of Shape Similarity Using Gaussian Functions. *J. Chem. Inform. Comput. Sci.* **1993**, *33*, 112–16.
- (25) Nichols, D. E.; Cassady, J. M.; Persons, P. E.; Yeung, M. C.; Clemens, J. A.; Smalstig, E. B. Synthesis and Evaluation of *N,N*-Di-*n*-propyltetrahydrobenz[*f*]indol-7-amine and Related Congeners as Dopaminergic Agonists. *J. Med. Chem.* **1989**, *32*, 2128–2134.
- (26) Hoffman, R. V.; Johnson, M. C.; Okonya, J. F. Synthesis and Reactions of 3-(Nosyloxy)-2-keto Esters. *J. Org. Chem.* **1997**, *62*, 2458–2465.

JM060302X